# Dispersion of ordered stripe phases in the cuprates

R. S. Markiewicz
*Department of Physics and Barnett Institute, Northeastern University, Boston, Massachusetts 02115*
(Received 8 November 1999; revised manuscript received 28 January 2000)

A phase-separation model is presented for the stripe phase of the cuprates, which allows the doping dependence of the photoemission spectra to be calculated. The idealized limit of a well-ordered array of magnetic and charged stripes is analyzed, including effects of long-range Coulomb repulsion. Remarkably, down to the limit of two-cell-wide stripes, the dispersion can be interpreted as essentially a superposition of the two end-phase dispersions, with superposed minigaps associated with the lattice periodicity. The largest minigap falls near the Fermi level; it can be enhanced by proximity to a (bulk) van Hove singularity. The calculated spectra are dominated by two features: this charge stripe minigap plus the magnetic stripe Hubbard gap. There is a strong correlation between these two features and the experimental photoemission results of a two-peak dispersion in $La_{2-x}Sr_xCuO_4$ and the peak-dip-hump spectra in $Bi_2Sr_2CaCu_2O_{8+\delta}$. The differences are suggestive of the role of increasing stripe fluctuations. The 1/8 anomaly is associated with a crossover from magnetic-dominated to charge-dominated stripes. A model is proposed for the limiting minority magnetic phase as an isolated two-leg ladder.

## I. INTRODUCTION

Evidence for stripe phases in the cuprates continues to grow. Particularly in the $La_{2-x}Sr_xCuO_4$ (LSCO) family, a convincing case for (predominantly dynamic or disordered) stripes can be made, based on elastic and inelastic neutron scattering,[1–5] NMR, and nuclear quadrupole resonance (NQR).[6,7] In other systems, the evidence is more ambiguous. In $YBa_2Cu_3O_{7-\delta}$ (YBCO), there is now[8,9] clear evidence for incommensurate modulation of the inelastic magnetic neutron scattering near $\vec{Q}=(\pi,\pi)$, but so far only in underdoped $YBa_2Cu_3O_{6.6}$. Balatsky and Bourges[10] find a broad commensurate peak, but the width of the peak scales with doping in exactly the same way as the incommensurability in LSCO, suggestive of an unresolved underlying incommensurability in YBCO, as well. Also, de Lozanne[11] finds direct scanning tunnel microscope (STM) evidence for incommensurate modulations (parallel to the chains) with a similar periodicity to the neutron data. Mook[12] has reported similar incommensurate neutron peaks in $Bi_2Sr_2CaCu_2O_{8+\delta}$ (BSCCO). Potentially stripe-related phonon anomalies have been reported in both LSCO (Ref. 13) and YBCO.[14] Doping with Zn seems to stabilize the stripe phase.[15] Photoemission evidence[16,17] for stripes has been controversial.[18,19]

Over the same doping regime, there is also evidence for a pseudogap, and it is an important problem to understand how both pseudogap and stripes can coexist. In particular, photoemission finds a dispersion consistent with the two-dimensional (2D) energy bands, whereas in the stripe phase the magnetic stripes should be insulating, leading to a one-dimensional (1D) dispersion along the charged stripes.

The presence of stripe phases raises important issues of how energy dispersion and even Fermi surfaces can be well defined concepts in the presence of fluctuating stripes. An important insight into this problem is the finding by Salkola, Emery, and Kivelson (SEK),[20] and Seibold *et al.*[21] that a well-defined average dispersion persists even in the presence of strongly fluctuating stripe order. The present paper analyzes a phase separation scenario, modeling the stripes as associated with free-energy minima at two characteristic hole densities. This is consistent with a number of calculations[22–26] which find that the stripes are associated with very sharp density variations, and allows the doping dependence of the stripes and the resulting photoemission spectrum to be analyzed.

It is found that long-range stripe order can persist even in the presence of Coulomb interactions. The resulting dispersion is clearly recognizable as a superposition of the magnetic and charged stripe dispersions, with superimposed minigaps due to the stripe order. These dual dispersions provide a natural interpretation for the experimentally observed photoemission dispersions, tying together results on LSCO, BSCCO, and $Sr_2CuO_2Cl_2$ (SCOC). In the model, the 1/8 anomaly can be understood as a form of quantum critical point (QCP), associated with a crossover between a magnetic stripe dominated regime and a charged stripe dominated regime. Within the latter regime, the $(\pi,\pi)$ spin gap in YBCO is related to the behavior of a two-leg ladder (isolated magnetic stripe).

Remarkably, within the charge stripe dispersion, a clear signature of the two-dimensional Van Hove singularity (VHS) persists, down to the limit of a single, two-Cu-wide stripe. There is a strong coupling of the minigaps with this VHS, leading to a *stripe-induced VHS splitting*. The doping dependence of this splitting closely resembles that of the pseudogap.

The paper is organized as follows. Section II shows that a low hole doping of the charged stripes, $x_0 \sim 0.25$, is not only compatible with experiment, but also makes sense theoretically, in terms of kinetic-energy stabilized stripes. The models for the magnetic and the charged stripes are introduced in Sec. III, along with a discussion of long-range Coulomb interaction. Section IV gives the results of the stripe calculations, which self-consistently determine the hole distribution. The doping dependence of the dispersion is presented for

 

varying strengths of Coulomb repulsion. Finally, the effect of an additional (ferromagnetic) interaction on splitting the VHS degeneracy on the charged stripes is discussed. In Sec. V, these results are compared to experiment, and a consistent model of the photoemission in LSCO and BSCCO is presented. The 1/8 anomaly is interpreted as a ''duality crossover,'' from a phase of majority magnetic stripes with charged domain boundaries to the dual phase. Section VI studies the properties of a phase with minority magnetic stripes, showing how the doping dependence of the spin gap in YBCO can be understood. Possible explanations are also presented for the saturation of the incommensurability $\delta$ vs $x$ found by Yamada *et al.*[2]

Section VII includes discussions of the interpretation of the peak-dip-hump structure in BSCCO, the stripe-VHS spitting pseudogap, and illustrations of Fermi surfaces and remnant Fermi surfaces in the stripe phase. The principal conclusions of this work are summarized in Sec. VIII.

## II. FRACTIONALLY OCCUPIED STRIPES

### A. Comparisons with other oxides

Stripe arrays have now been found in a number of oxides, most notably nickelates and manganites. The similarities of cuprates with nickelates are particularly close: in both systems, the charged stripes act as antiphase boundaries for the magnetic stripes, and in both, the charge order arises at higher temperature than the magnetic order.[1,27] The nickelate stripes run diagonally (with respect to the Ni-O-Ni bonds); this is also true of the LSCO stripes, in the spin-glass regime,[28] $x \sim 0.04$–$0.06$. However, in the superconducting regime, $x > 0.06$, the cuprate stripes are generally horizontal and vertical.

One striking difference is that in the nickelates and manganites, the charged stripes correspond to integer doping (one hole per Mn or Ni), leading to simple patterns[29,30] of commensurate stripe arrays. There are prominent phase transitions at rational fractions, 1/2, and 1/3, corresponding to holes on every $n$th row, with evidence for commensurability locking in between (i.e., the 1/3 phase persists in an extended doping range about $x = 1/3$.) Consistent with integer filling, the phases are all insulating.[29] In contrast, in the cuprates the phases are all conducting or weakly localized, and the only fraction which appears prominently is 1/8.

In the present paper, a simple explanation is proposed for this distinction. The charged stripes are fractionally doped, with approximately 1/4 hole per Cu (hence explaining the finite conductivity). The magical 1/8 doping would then correspond to the simplest ''commensurate'' pattern of these stripes.

The stability of the stripe phase decreases in the sequence manganites, nickelates, cuprates. Thus, while there are beautiful electron microscopic images of long-range stripe order in the manganites,[30] stripes in the cuprates are mainly fluctuating, with only short-range order. Within the present model, this pattern is readily understood, since the charged stripes are stabilized by charge-density wave (CDW) instabilities; this is similar to models for the nickelates and manganites.[31] The strength of this instability can be estimated by comparing the strength of electron phonon coupling, which follows the same sequence: manganites (with well-defined Jahn-Teller polarons), nickelates,[32] cuprates. It is only in the cuprates where the interaction is so weak that a fractional occupation can be stabilized, and it is only in the cuprates that the stripe formation is so weak that superconductivity can successfully compete.

### B. Origin of fractional occupation

Hartree-Fock calculations[22] of the $tJ$ model find that the holes condense onto domain walls between antiferromagnetically ordered domains, producing fully occupied charge stripes—one hole per Cu. However, neutron diffraction[1] finds a charge modulation of periodicity four Cu atoms at $x = 0.125$, which implies only 1/2 hole per cell. Tranquada *et al.*[1] suggested a model for the charged stripes, based on their experience with stripes in nickelates. The hole-doped stripes are one cell wide, and have a hole on every other site. A microscopic model for such a domain wall can be derived[33] by incorporating a charge-density wave (CDW) instability along the stripes, treating them as one-dimensional metals. However, such states with integral hole doping are likely to be insulators, as is the case in the stripe phases of the nickelates,[29] whereas the cuprates are either conducting or weakly localized.

Moreover, fractional hole occupation would seem to be more natural for the $tJ$ and Hubbard models, since the energy of doped holes is lowered by finite hopping $t$ in a partially filled band. Visscher[34] and Nagaev[35] showed that the holes enhance their kinetic energy by creating local ferromagnetic domains (ferrons) in which they are free to hop. This leads to a preferred hole density $x_f$ inside the ferron domain. In a two-dimensional, $tJ$ version of the model (letting $\hbar^2/2m \rightarrow ta^2$, with $a$ the lattice constant),

$$x_f = \sqrt{\frac{zS^2J}{\pi t}} \simeq 0.334, \tag{1}$$

with $z = 4$ the number of nearest neighbors of a given Cu, and I have assumed $J/t = 0.35$. A similar result was found by Nayak and Wilczek.[36] Nagaev's model is a large-$S$ theory, and Emery and Kivelson[37] extended it to $S = 1/2$, although they did not address the issue of $x_f$. Auerbach and Larson[38] showed that a single doped $S = 1/2$ hole will spread out over a ferromagnetic domain covering five lattice sites, suggesting a comparable value for $x_f, > 0.2$ holes per cite, on average (since the hole has a higher probability of being on the central atom). Recent density-matrix renormalization-group (DMRG) calculations of the $tJ$ model by White and Scalapino (WS) (Ref. 39 and 40) find charged stripes which are two Cu's wide, with an average hole doping of 0.25 hole per Cu on the charged stripes (although WS suggest that the relevant quantity is the net charge per unit length along the stripe, 0.5 hole).

Since the charged domains are stabilized by the hole kinetic energy, it is plausible that enhancing the kinetic energy could enhance the stability of the hole-doped stripes. Thus, in a generalized Hubbard model, with next-nearest-neighbor hopping $t'$, it is found that a macroscopic ferromagnetic phase is stabilized in the vicinity of the van Hove singularity (VHS).[41] Moreover, an extended Hartree-Fock analysis[25] finds phase separated states smoothly evolving between the

antiferromagnetic (AFM) and ferromagnetic (FM) regions, from a single magnetic polaron to FM stripes to a uniform FM phase.

However, such ferromagnetic domains have not been observed in the cuprates. Nevertheless, there are alternative VHS routes to fractionally occupied stripes. The large density of states (DOS) associated with a VHS can drive a large number of competing electronic instabilities,[42,43] and it was suggested early that this could be the origin of nanoscale phase separation in the cuprates.[44] In particular, it was demonstrated that strong electron-phonon coupling could stabilize a charge-density wave phase near the VHS.[44,45]

### C. Viability of VHS models

In any model of stripe phase formation based on Fermi surface features, there is a fundamental question of self-consistency: do the features persist in the limit of an isolated stripe? Can one still recognize bulk features of the band structure and Fermi surfaces of the phases forming the stripe array? This is one of the main issues that this paper resolves: even in the limit of nanoscopic stripes, the band structure is recognizably a superposition of the structures of the two end phases. The main role of stripe order is to introduce miniband gaps into this structure.

In the particular case of the VHS's, there were a number of preliminary indications which suggested such an affirmative answer. First, SEK (Ref. 20) found that an average dispersion persists in the presence of fluctuating stripes; the resulting ''flat bands'' are a signature of the VHS. Second, within a group theoretical $[SO(6)]$ model,[43] the van Hove instabilities all remain well defined on a single plaquette of $2\times 2$ Cu atoms, so *a fortiori* they should remain well defined on a two-leg ladder. Indeed, Lin, Balents, and Fisher[46] found an $SO(8)$ group controlling the physics of the two-leg ladder. When one eliminates[47] certain one-dimensional operators (which break the $k\rightarrow -k$ symmetry along the ladder), one is left with the same $SO(6)$ group introduced earlier for the VHS. Such a correspondence would fail for a single-leg ladder.

Hence the present model is restricted to stripes which are an even number of cells (or Cu atoms) wide. This point was previously postulated for the magnetic stripes, in terms of spin gaps associated with even-legged ladders.[48] Moreover, WS find two-Cu-wide charged stripes in their DMRG calculations.[39] With this assumption, it is found that a VHS-like feature can be clearly resolved near the Fermi level in the stripe phases. Moreover, the stripes provide an interesting mechanism for VHS splitting—minigaps—which can generate a pseudogap with the correct doping dependence.

## III. MODELING THE STRIPES

While the stripes are likely to be strongly fluctuating, the band-structure modifications should be strongest, and can be analyzed in most detail, in an ordered stripe phase. Hence the present calculation assumes perfectly ordered stripe phases to describe this ''worst case'' scenario. It will be assumed that there are two preferred hole densities, $x\sim 0$ on the magnetic stripes, and $x_0\sim 0.25$ holes per Cu on the hole-doped stripes. Coulomb effects lead to additional charge relaxation, and a more uniform distribution of charge (see Sec. III D).

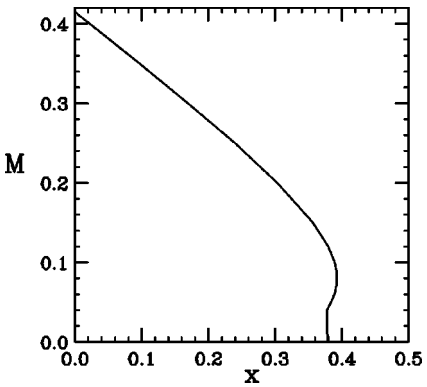


FIG. 1. Doping dependence of magnetization in the SDW model.

### A. Model for the magnetic stripes

In the insulating phase, a variant of the spin-density wave (SDW) model studied by Schrieffer and co-workers[49,50] is used. This model works surprisingly well in the large-$U$ limit,[51] reproduces the spin-wave spectrum of the Heisenberg model, and has served as the basis for a number of extended treatments of correlation effects.[52–55] For realistic parameters $(t,t',U)$, the model has a Mott-Hubbard gap of 2 eV, and can reproduce the dispersion found in the oxyclorides;[56,57] see the Appendix.

The dispersion of the one-band model can be written

$$\epsilon_k=-2t(c_x+c_y)-4t'c_xc_y, \tag{2}$$

with $c_i=\cos k_i a$. Writing $\epsilon_\pm=(\epsilon_k\pm\epsilon_{k+Q})/2$, the eigenvalues in the presence of a Hubbard $U$ become

$$E^\pm=\epsilon_+\pm\sqrt{\epsilon_-^2+\overline{U}^2}, \tag{3}$$

where $\overline{U}=Um_Q$. In the limit $\overline{U}\gg t$, the lower Hubbard band may be approximated

$$E^-=-\overline{U}-4t'c_xc_y-J(c_x+c_y)^2, \tag{4}$$

with $J=2t^2/\overline{U}$. The parameters can be determined by fitting to the observed photoemission dispersion in SCOC. For simplicity, one can use analytical expressions for the parameters at three $k$-space points: $E^-(\pi/2,\pi/2)=-\overline{U},E^-(\pi,0)=-\overline{U}+4t',E^-(0,0)=-4t'-\sqrt{\overline{U}^2+16t^2}$ [Eq. (4) is not sufficiently accurate for this purpose]. The fit yields $t=325$ meV, $\overline{U}/t=2.5$, and $\tau=2t'/t=-0.552$. Solving the gap equation at half filling, this value of $\overline{U}$ corresponds to $U/t=6.03$, $M_Q(x=0)=0.414$ (Fig. 1), or 83% of the classical value.

For these parameters, $M(x)$ is multivalued for $x\geqslant 0.38$. This implies that the magnetic to nonmagnetic transition is first order. This is discussed further in the Appendix. However, this density is rather higher than expected for charged stripes. In LSCO, the VHS splitting seems to terminate near $x=0.26$,[58,59] and similar results are found below for YBCO. In a number of models,[45,41] the AFM instability is replaced by a second instability, driven by splitting the VHS degeneracy. Note that the bare $(U=0)$ VHS falls at $x=0.25$ for $\tau=-0.559$, very close to the value needed to explain the dispersion in the insulating phase.

If $M_Q$ is interpreted as the long-range antiferromagnetic order parameter, then the model does a poor job in describing the temperature and doping dependence of the Néel transition,[60] $T_N$, yielding $T_N \sim U/4$. Figure 1 shows that, while $M_Q$ is strongly renormalized by doping, the mean-field theory underestimates the rapidity of the falloff of $T_N$ with $x$. However, the mean-field results are best reinterpreted as representing *short-range order*—the magnetic fluctuations—and hence the renormalization of the *splitting* into upper and lower Hubbard bands. In this case, the mean-field calculations are in good agreement with exact diagonalization calculations.[61] The fact that the gap is much smaller in the doped phase is consistent with the experimental observation[62] that the upper Hubbard band rapidly disappears with doping.

### B. Model for the charged stripes

It is assumed that the hole-doped stripes are stabilized by splitting the VHS degeneracy, at the doping $x_0 \sim 0.25$ where the VHS falls at the Fermi level. An earlier slave boson calculation[45] demonstrated that electron-phonon coupling could provide that stabilization energy, even in the presence of strong correlation effects. A ferromagnetic interaction[41] can produce similar splitting.

While the earlier electron-phonon calculation involved a three-band model, here a simpler one-band model will be adopted. A parametrized form of the free energy vs doping found in the self-consistent calculation[45] will be assumed, to stabilize the stripe phase. It is convenient at present to *not* introduce any mechanism to split the VHS degeneracy. This allows a definitive answer to an important question: can evidence for the VHS still be found in the presence of a well-defined stripe phase? The answer is a clear yes: the resulting dispersion is a superposition of the magnetic dispersion and the charged stripe dispersion, with recognizable VHS feature. What is more, the stripe phase minigaps provide a *different mechanism of VHS splitting*, with a doping dependence comparable to the experimental pseudogap.

A very simple doping dependence of the parameters is assumed. From Eqs. (2)–(4), for finite $U$, $t$ is renormalized by a factor $t/Um_Q$, Fig. 1, so the increase of $t$ with doping is accomplished by the decrease in $m_Q$, the ordered moment. We will thus make a simple ansatz that the only effect of doping is to renormalize

$$m_Q \rightarrow m_Q(1 - x/x_0). \tag{5}$$

Since the stripes are predominantly near the limiting states $x=0$, $x_0$, the detailed nature of the intermediate states is relatively unimportant. As noted above, Eq. (5) neglects the gap on the charged stripe; in Sec. IV D, a ferromagnetic interaction will be included on the charged stripes, to show that the VHS splitting is preserved in the striped phase.

### C. Free-energy minima

To stabilize the stripe densities at the values $x=0$ for magnetic stripes, and $x=x_0=0.25$ for the charged stripes, the following free energy is introduced, based on the results of slave boson calculations for the three-band model:[45]

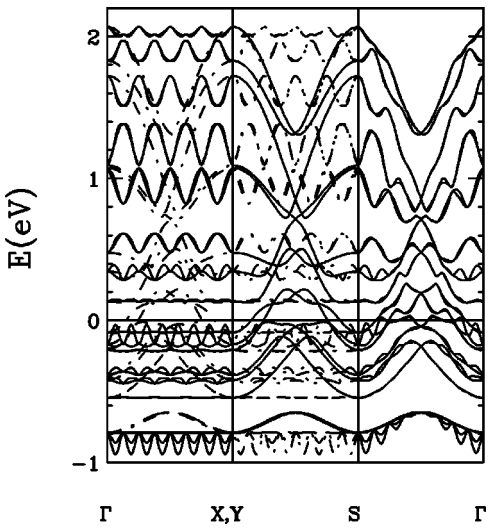


FIG. 2. Dispersion of 2,6 structure. Solid lines $\Gamma \rightarrow X=(\pi,0) \rightarrow S=(\pi,\pi) \rightarrow \Gamma$; dot-dashed lines $\Gamma \rightarrow Y=(0,\pi) \rightarrow S$. Here, $Y$ is along the stripes, $X$ is across them.

$$f_0(x) = \mu_0 x \left(1 - \frac{x}{x_0}\right)^2, \tag{6}$$

for $x>0$. (At $x=0$ there is a cusplike minimum, associated with the Mott gap in the chemical potential.) Equation (6) was fit[63] to the free energies calculated in a three-band slave boson model for competing magnetic (flux phase) and charged (CDW) phases, Fig. 2 of Ref. 45. (Note that there is an error in the caption of that figure: the correct CDW coupling is $V_{ep}=0.6$ eV.)

Equation (6) is a convenient form for parametrizing the confining potential of a striped phase. It has only two parameters, $x_0$ and $\mu_0$, or equivalently, $f_m = 4\mu_0 x_0/27$, the maximum free-energy barrier, at $x_0/3$. In the present stripe phase calculations, these parameters are taken as $x_0=0.25$ and $\mu_0 = 0.312$ eV, or $f_m = 11$ meV. This value corresponds to $V_{ep}=0.6$ eV of Ref. 45, and allows us to see that even a relatively modest confining potential can stabilize the stripe phase against the Coulomb potential. This free energy corresponds to an additional chemical potential

$$\mu(x) = -\mu_0 \left(1 - \frac{x}{x_0}\right)\left(1 - \frac{3x}{x_0}\right) \tag{7}$$

for $x>0$. In the calculations, this $\mu(x)$ is added to the potential on each row, and the local density adjusted until self-consistency is attained.

At $x=0$, $\mu$ has a discontinuity, the Mott-Hubbard gap. Hence, at this point, the Fermi level can take on any value inside the gap. To model this in a computationally stable manner, the discontinuous step in $\mu$ is replaced by a linear ramp, connecting the values of $\mu$ at $x=-0.01$ and $x=+0.01$, and assuming $\mu(x=-0.01) = -\mu(x=+0.01)$. Thus, when the calculation finds $|x|<0.01$, it generally implies that the Fermi level is in the gap of the magnetic stripes. However, due to hybridization with holes in the charged stripes, it is possible to have a well-defined Mott gap, with a small doping $x>0$ on the magnetic stripes (typically, $x \leq 0.05$).

TABLE I. Madelung matrices.

| $K^m_{ij}$ | $j=2$ | 3 | 4 |
|---|---|---|---|
| $K^6_{2j}=$ | −0.4110 | 0.5365 | 0.347 |
| $K^6_{3j}=$ | −0.3466 | 0.4721 | 1.230 |
| $K^6_{4j}=$ | −0.8831 | 0.8831 | 1.702 |
| $K^4_{2j}=$ | −0.3082 | 0.6951 | |
| $K^4_{3j}=$ | 0 | 1.082 | |
| $K^2_{2j}=$ | 0.1256 | | |

### D. Madelung energies of stripes

We will assume for simplicity that all stripes, both magnetic and charged, are an even number of cells wide. This means that only a relatively small number of stripe configurations are involved in the doping range of interest. For instance, labeling the stripe configuration by $m,n$, where $m$ is the width of a magnetic stripe and $n$ the width of a charged stripe, we will explore in detail the pure phases $m,n=6,2$ ($x=x_0/4\simeq 0.0625$, if $x_0\simeq 0.25$), 4,2 ($x=x_0/3\simeq 0.0833$), 2,2 ($x=x_0/2\simeq 0.125$—the 1/8 phase), 2,4 ($x=2x_0/3\simeq 0.167$), and 2,6 ($x=3x_0/4\simeq 0.1875$). Intermediate dopings would correspond to mixed phases. For each of these phases, we assume that there can be different dopings on each row; by symmetry, there can be $(m+n)/2$ inequivalent rows for the $m,n$ phase.

In the presence of charging, it is the electrochemical potential $\mu_e$ and not the chemical potential $\mu$ which is constant. For electrons, $\mu_e=\mu-eV$, where $V$ is the electrical potential. Given the average hole density on each row, $V$ can be calculated as a Madelung sum. For each configuration, the Madelung sum can be calculated for each row. Actually, since the overall chemical potential must be adjusted to fix the total hole density, all that need be calculated is the difference in Madelung potential between the different rows. This is calculated by assuming a pure Coulomb interaction, screened by a static dielectric constant, $\epsilon$. The on-site term is neglected, having already been included as $U$.

The various Madelung constants can be expressed as follows. For the (6,2) stripe, we label the rows 1,2,3,4, with 4 = the charged stripe, and 1 (3) = the magnetic rows farthest from (nearest to) row 4. Let $V_i$ be the Madelung potential for the $i$th row, $\tilde{V}_i=(V_i-V_1)x_0$, $x_i$ the hole doping of the $i$th row, and $\tilde{x}_i=(x_i-x_1)/x_0$. Then

$$\tilde{V}_i=V_0\sum_j K_{ij}\tilde{x}_j, \tag{8}$$

where the $K^m$ matrices have been calculated numerically, with results listed in Table I, for the cases $(m,2)$, $m=2,4,6$. The constant $V_0=2x_0e^2/(\epsilon a)=0.914eV/\epsilon$, for $x_0=0.25$.

The stripe phase is stable only if the dielectric constant is large enough: recent calculations[64] suggest $\epsilon>5$ is sufficient. The large static dielectric constant of the cuprates, $\sim$40–80,[65] is a sign of strong electron-phonon coupling. This large coupling makes it difficult to accurately estimate the strength of the Coulomb interaction. The dc dielectric constant will be anisotropic and, most probably, dispersive, on the length scale of the stripes. Since interlayer contributions to screening can be important (e.g., apical oxygens, bilayer coupling), this is one parameter which could easily have a strong material dependence.

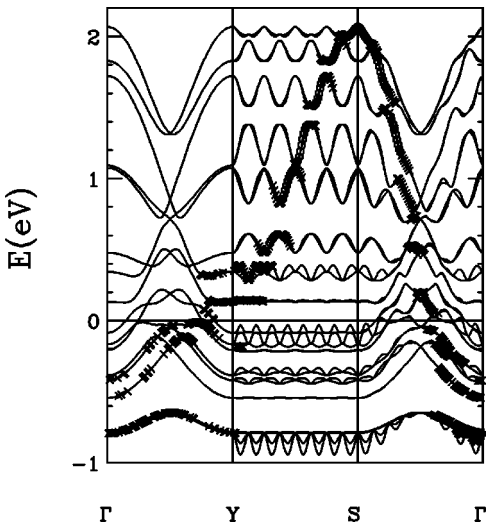


FIG. 3. Dispersion of 2,6 structure, but with structure factors.

While the above procedure should approximately capture the long-range part of the Coulomb interaction, it will likely overestimate the hole-hole repulsion for nearest neighbors. This can be thought of in terms of a correlation hole having two components. First, we are assuming that a hole on a given site interacts with a fractional hole (the average doping) on all other sites. Clearly, part of the hole population on the nearest-neighbor sites is actually generated by the hopping of the given hole, hence should not be counted in the Madelung sum. Moreover, there is likely to be a real correlation hole, as neighboring charges readjust to avoid the given hole. However, these terms are associated with CDW formation, which will not be dealt with explicitly here.

## IV. RESULTS

### A. Structure factor effects

Figure 2 illustrates the band dispersion for a 2,6 structure ($x=0.1875$), in the absence of long-range Coulomb effects. The hole doping on each layer is self-consistently adjusted to allow for inter-row hopping processes, and the Fermi level is adjusted to account for the overall doping. In the absence of long-range Coulomb effects, the doping is close to the nominal values. Numerical results will be discussed in the following subsection, which will show how they are modified by Coulomb interaction.

The large number of bands is rather deceptive. It is equal to the number of Cu atoms in the large unit cell, doubled since the up and down spin bands are not degenerate. There would be the same number of bands *even if there were no stripes*. But in this case, only one band would satisfy Bloch's theorem. This band can be determined by looking at the structure factor—the overlap of the corresponding wave functions with $e^{i\vec{k}\cdot\vec{r}}$. Similarly, when stripes are present, the same structure factor determines which bands will be seen by photoemission. This is illustrated in Fig. 3, where the circles indicate a weight greater than 0.5, and the ×'s a weight between 0.5 and 0.1. For greater clarity, only the dispersions along $\Gamma\rightarrow Y\rightarrow S$ are shown. The dispersions along $Y$ (parallel

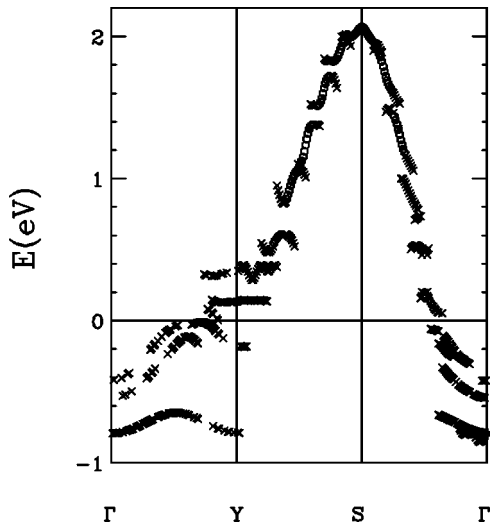


FIG. 4. Dispersion of 2,6 structure, parallel to the stripes.

to the stripes) and $X$ (transverse to the stripes) are shown in Figs. 4 and 5, respectively. The resulting weights reveal a simple result: the envelope of the bands is approximately a superposition of the two limiting bands, at half filling and at optimal doping, with considerable fine structure associated with minigaps.

In the presence of stripes, the dispersion should be quasi-one-dimensional. This is clearly seen in Fig. 2, where the dispersion along $\Gamma \rightarrow Y$ ($\Gamma \rightarrow X$) closely resembles that along $X \rightarrow S$ ($Y \rightarrow S$). However, with the structure factors included, the dispersions are quite distinct. Nevertheless, the minigaps are most prominent in the dispersions perpendicular to the stripes, $\Gamma \rightarrow X$ (Fig. 5), and $Y \rightarrow S$ (Fig. 4).

### B. Coulomb interaction

The doping dependence of the dispersion is shown in Fig. 6 (no Coulomb effects) and Fig. 7 (moderate screening, $\epsilon = 15$). The curves show the dispersions for a series of dopings, from $\Gamma \rightarrow X \equiv (\pi,0) \rightarrow S \equiv (\pi,\pi)$. While the fine structure (minigaps) is strongly doping dependent, *the overall dispersion is not*, and is essentially identical to the dispersion of the uniform end phases. This is exactly what would be expected for *macroscopic* phase separation, even though at crossover the charge stripe is only two cells wide.

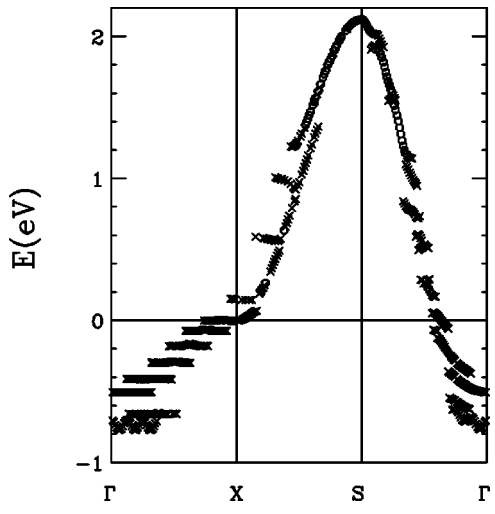


FIG. 5. Dispersion of 2,6 structure, transverse to the stripes.

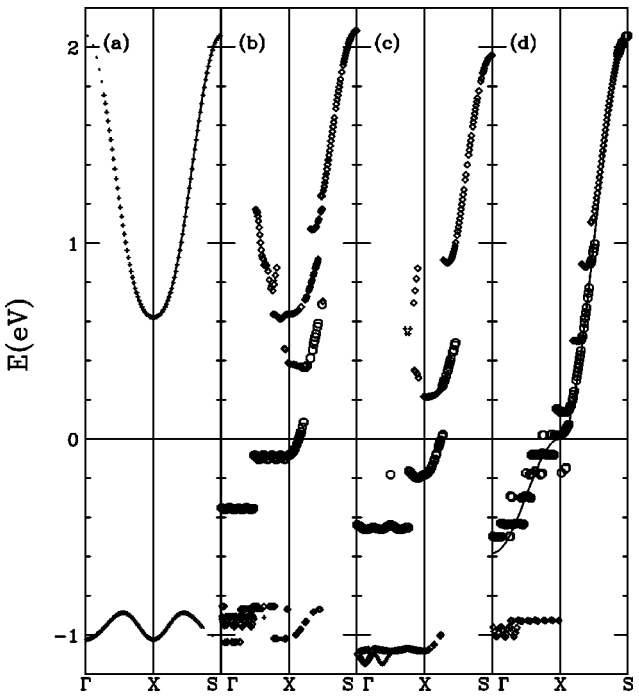


FIG. 6. Total dispersion in the absence of Coulomb repulsion, from $\Gamma \rightarrow S$ for dopings: $x = 0$ (a), 0.0625 (b), 0.125 (c), 0.1875 (d), and 0.25 [solid line in (d)]. Data in (a) were shifted upward by 0.16 eV.

The figures show that the dispersion is largely a superposition of two sets of bands: one for the insulating magnetic stripes, one for the charged stripes. The small $+$'s (large circles) indicate $\geqslant 80\%$ of the wave function is on the mag-

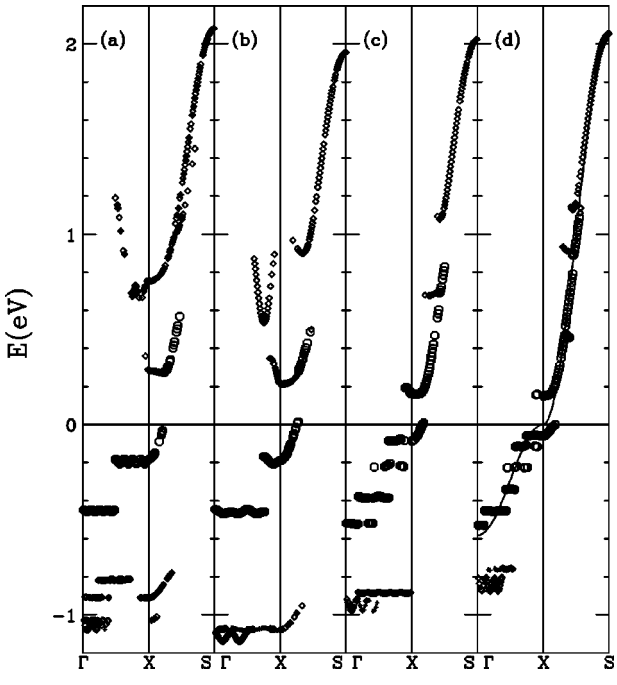


FIG. 7. Total dispersion corrected for charging ($\epsilon = 15$) from $\Gamma \rightarrow S$ for dopings: $x = 0.0625$ (a), 0.125 (b), 0.167 (c), 0.1875 (d), and 0.25 [solid line in (d)].

netic (charged) stripe; the small diamonds indicate a mixture of both. Note that there is strong overlap in the region of the upper Hubbard band, while the magnetic lower Hubbard band (LHB) remains well defined at all dopings, and the charged stripes fill in the gap as doping increases.

It should be noted that once the charged stripes are reduced to two cells wide, at $x=0.125$, the dispersion remains nearly unchanged as the doping is further reduced (e.g., at $x=0.0625$). Hence an important aspect to understanding the strongly underdoped stripe phases will be to develop a good model for these limiting, two-cell stripes. As discussed below, there is an analogous magnetic stripe beyond the percolation crossover, which can be modeled as a two-leg ladder.

Inclusion of Coulomb interaction leads to fairly modest changes in the dispersion. Careful inspection of Figs. 6 and 7 reveals that charging effects push holes onto the magnetic layers, shifting the lower Hubbard band toward the Fermi level and causing it to more fully hybridize with the charged layers. With reduced screening ($\epsilon=5$) the bottom of the charged band actually falls below the magnetic lower Hubbard band. The layers near the Fermi level remain predominantly associated with the charged layers, so we may still loosely speak of charged bands and magnetic bands. Note that in every case, the Fermi level lies within the miniband closest to the van Hove singularity. This provides a *different mechanism* for the opening of the pseudogap, as will be discussed further below.

Even in the absence of Coulomb interaction, the carrier density in a given row deviates somewhat from the free-energy minima—here taken as $x=0,0.25$—due to the finite hopping probability. For the 2,6 structure, Figs. 2–4, the magnetic layers have $x=0.025$, and for the charged layers, moving away from the magnetic layer, the hole doping is 0.25, 0.24, and 0.24. Adding the Madelung potential raises the energy of the hole-doped stripes, and requires a shift of the Fermi energy to compensate. However, since the magnetic stripes are gapped, this shift makes little difference to the hole population on these stripes, the corresponding layer populations being 0.026, 0.255, 0.25, and 0.22, for $\epsilon=15$ (Fig. 7). For larger Coulomb interaction, the deviation becomes greater (Fig. 8). The data display an interesting evolution: superimposed on a trend toward greater homogeneity, there is also a tendency to evolve into a (2,2) state. This can be understood from Table I: the Coulomb effects are smallest for this state, since the phase separation is restricted to the finest scale.

This result is of potential relevance for LSCO: it is found experimentally that the incommensurability saturates near 1/8 doping—here the crossover where the (2,2) phase is stable. The saturation could simply mean that for LSCO, the Coulomb effects are large enough that the system locks into the (2,2) phase for all higher dopings.

There is a striking asymmetry about 1/8 doping: in the (6,2) phase, Coulomb interaction makes very little difference. This is because of the sharp cusp instability at half filling, which keeps the hole doping fixed near zero in the magnetic stripes, whereas the shallower potential minimum near optimal doping allows more substantial density fluctuations.

These results will be discussed further in a later section. Two points are worth mentioning: first, the incommensurability saturation has so far only been observed in LSCO; and second, LSCO closely resembles the other cuprates in the doping range up to 1/8, but for higher doping, $T_c$ saturates at a much lower value.

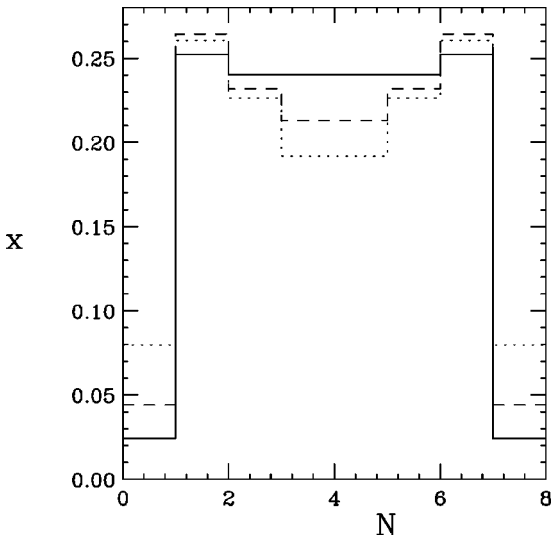


FIG. 8. Hole distribution on rows (labeled by $N$) of the 2,6 structure, for $\epsilon=\infty$ (i.e., no Coulomb interaction—solid line), 15 (dashed line), or 5 (dotted line).

### C. Minigaps

Figure 7 shows the evolution of the minigaps with doping. A simple model provides a semiquantitative explanation of these results. The dispersion along $(0,0)\rightarrow(\pi,0)$ is discretized into $n$ levels for $n$-Cu-wide charge stripes. This bandwidth is $4(t+2t')\simeq 584$ meV. If the minibands are equally spaced, the average gap should be $584/(n-1)$ meV. Actually, the net bandwidth changes some with doping, so a better formula is

$$\Delta_{av}=\frac{584\ \text{meV}}{n} \tag{9}$$

$=292$ $(n=2)$,146 (4), or 97 (6) meV, to be compared with average values (Fig. 7) of 260, 147, and 94 meV, respectively. For the dispersion along $(0,\pi)\rightarrow(\pi,\pi)$, the same bands are present, but shifted by the dispersion along $Y$, and with total bandwidth $4(t-2t')$.

For fluctuations in the stripe spacing, there will be a tendency to average over the various dispersions in Fig. 7. This will tend to wash out most of the minigaps, since they are shifted in energy as the stripe width changes. However, since there is always one gap present near the Fermi level, this gap should survive averaging. For the uniform stripe phases of Fig. 7, this ''pseudogap,'' or distance between the Fermi level and the nearest $(\pi,0)$ minigap edge, follows the same scaling as Eq. (9), $\Delta_p=364/n$ meV.

### D. Ferromagnetic stripes

Figure 7 shows that beyond the percolation crossover a clear remnant of the bulk VHS is visible in the striped phase dispersion. In Fig. 9, it can be seen that splitting this VHS degeneracy produces a clear pseudogaplike splitting of the

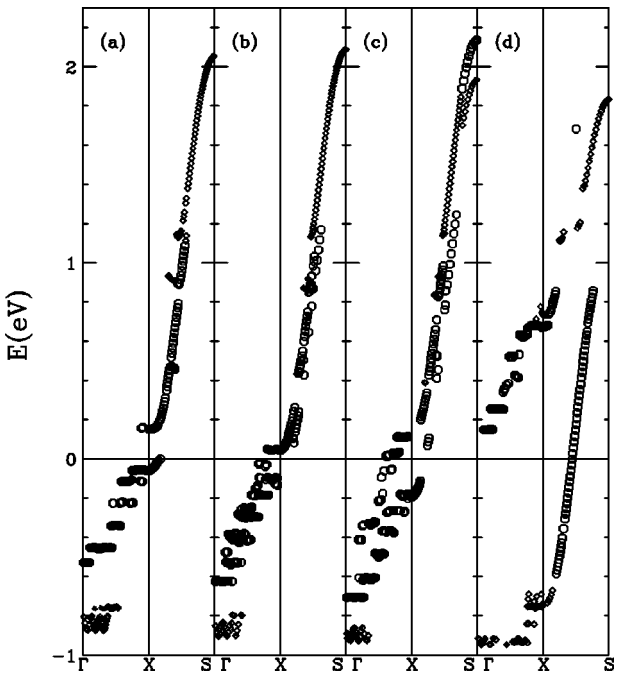


FIG. 9. Dispersion along $X$ for a ferromagnetic instability on the charged stripes, for $x=0.1875$ (2,6), and different degrees of magnetization $M$, as discussed in the text.

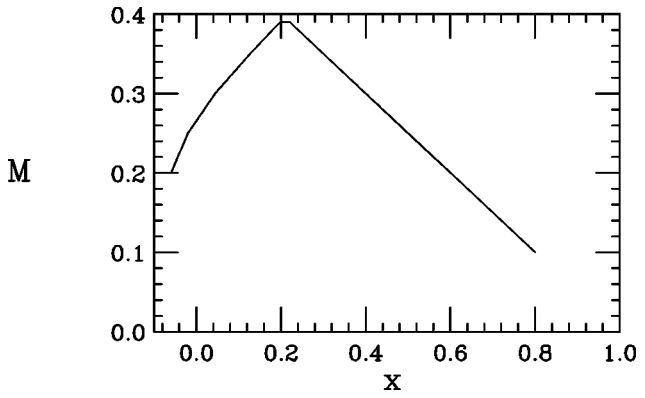


FIG. 10. Doping dependence of the magnetization $M$ for a ferromagnetic instability.

dispersion near $(\pi,0)$. It is this lowering of a large density of states that has been postulated to stabilize the charged stripes, and the figure clearly shows that the mechanism remains active even in the striped phase.

For the calculations in the figure, it was assumed that the antiferromagnetic phase is stable only up to a doping $x_0/3$, while for larger doping a ferromagnetic instability wins out. The ferromagnetic dispersion is also given by Eqs. (2)–(4), but with $q=(0,0)$ instead of $Q=(\pi,\pi)$. For the same value of $U$, the equilibrium $M$ has the form shown in Fig. 10, which was approximated by $M=0.4–0.5|x-0.2|$.

It should be noted that the doping dependence depends sensitively on the choice of parameters; these values are taken for illustrative purposes only. Figure 9(d) shows the dispersion of the self-consistent solution with the full $M(x)$, while the other frames show a reduced $M$ of 1/5 (c), 1/10 (b), or 0 (a). Since the parameters were chosen to have the VHS in frame (a) centered on the Fermi level, the pseudogap opens approximately symmetrically about the Fermi level.

This should not be taken as evidence that the charged stripes really are ferromagnetic, only as an example of yet another kind of instability that is driven by the VHS. The figure illustrates that one can distinguish different instabilities, but one must carefully analyze secondary characteristics, since the opening of the pseudogap near $(\pi,0)$ is common to a variety of instabilities. In the present instance, a ferromagnetic instability does not double the unit cell, so the ghost dispersion beyond $(\pi,0)$ is absent, in contrast to experiment [see Fig. 19(b) below]. Moreover, the splitting of the spin-up and spin-down bands should lead to extra structure most clearly seen (below the Fermi level) near $\Gamma$, which is not found experimentally.

## V. COMPARISON TO EXPERIMENT

### A. Photoemission in LSCO

The doping dependence of the photoemission spectra in LSCO (Ref. 66) is strikingly different from that in BSCCO.[67] In this section, it will be shown that *both* spectra can be interpreted in terms of stripe phases, with stronger fluctuation effects in BSCCO. The key observation, Fig. 7, is that stripes produce distinct dispersion features associated with the magnetic stripes and the charged stripes—which can be identified with the hump and peak features in superconducting BSCCO, and with similar features in LSCO.

Since most samples contain many stripe domains, the photoemission should be compared with a superposition of the $X$ and $Y$ dispersions (Fig. 11). The following features should be noted: (i) there is always a flat band pseudogap near $(\pi,0)$, which tends to shift further below the Fermi level with increased underdoping. (ii) The evolution with doping is not smooth: with increased doping, the magnetic band gradually fades away while a more metallic band grows in near the Fermi level. The overall doping dependence is quite similar to the experimental results of Ino *et al.*[66] (see particularly their Fig. 3), confirming the suggestion that stripes are better developed in LSCO than in BSCCO.

Figure 12 compares the $(\pi,0)$ photoemission peak positions for LSCO (Ref. 66) with the present calculations. Results for BSCCO (Ref. 68) are also shown; these will be discussed in the following subsection. In LSCO, there are two main features: one ($\times$'s) is near $-0.6$ eV, with a dispersion similar to that in the magnetic insulator SCOC, and with a nearly doping-independent binding energy. The second feature (open circles) is a gap close to $E_F$ with larger doping dependence. Qualitatively, these features are similar to the hump and peak features in BSCCO, but with larger binding energies. These two features can be correlated with two prominent gaplike features in the calculations: the magnetic gap associated with the lower Hubbard band on the magnetic stripes, and the charge stripe gap, associated with the miniband closest to the Fermi level. The calculated gaps are larger, since the energy scale has been chosen to agree with the magnetic gap in SCOC, yielding a value $-1.2$ eV at half filling, but the overall doping dependences are quite

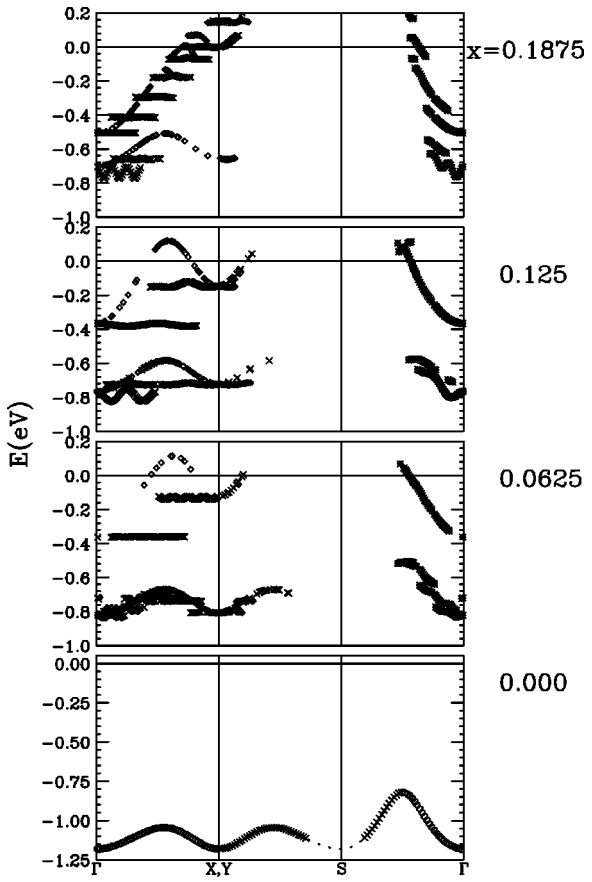


FIG. 11. Superposition of $X$ and $Y$ dispersions for, from bottom to top, $x = 0$, 0.0625 (6,2 structure), 0.125 (2,2), and 0.1875 (2,6).

similar to LSCO. This similarity is brought out most clearly by plotting the calculated gap values divided by two (diamonds and suns).

### B. Photoemission in BSCCO

#### 1. Below $T_c$

In BSCCO, there is a remarkable evolution of the photoemission with temperature, particularly on passing through $T_c$. Above $T_c$, the spectra are very broad, with a single broad peak near $(\pi,0)$ representing the normal-state pseudogap. Below $T_c$, the spectra sharpen and split into two features, commonly referred to as a ''peak'' near $E_F$, with a ''hump'' at lower energies, close to the normal-state pseudogap; between the peak and hump, there is a clear ''dip'' in intensity, below the level in the normal state. Recently, systematic studies of these features in both tunneling[69] and photoemission[68] were presented. Most strikingly, photoemission finds these two peaks in the same direction of $k$ space, a feature which is very suggestive of phase separation.

Here, it will be assumed that the photoemission is dominated by stripe effects, and the main role of superconductivity is to suppress fluctuations. (The clear sharpening of the spectra below $T_c$, even in a range away from any gaps, is demonstrated in Ref. 70.) The analysis will be in two parts. First, the low-$T$ spectra will be compared with those of LSCO. Then the role of fluctuations in producing the high-$T$ smeared spectra will be discussed.

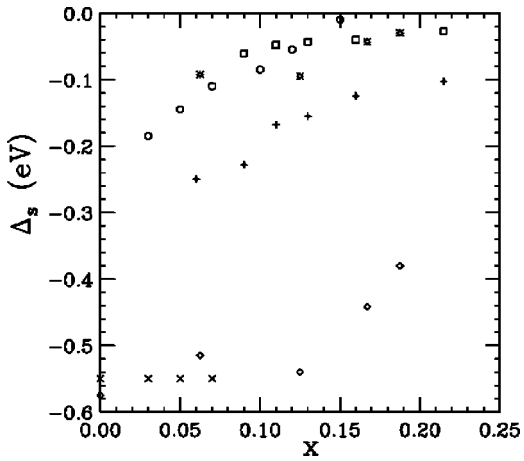


FIG. 12. Pseudogaps at $(\pi,0)$ in LSCO (Ref. 66) ($\times$'s, open circles) and BSCCO (Ref. 68) ($+$'s = hump, squares = peak) compared to calculated Mott gap (diamonds) and minigap (suns); the calculated values are reduced by a factor of 2. At the highest doping, the Mott gap does not show much intensity near $(\pi,0)$; what is plotted is energy of the corresponding dispersion nearest to $(\pi,0)$.

In Fig. 12 the low-temperature photoemission peaks[68] of BSCCO are compared to those of LSCO. The peaks (squares) are in reasonable agreement with the near-$E_F$ pseudogap in LSCO (circles), and with the calculated minigaps. On the other hand, the humps ($+$'s) are considerably closer to the Fermi level than the magnetic stripe feature in LSCO ($\times$'s); compared to theory, the overall offset is different, but the doping dependence is similar. Nevertheless, identification of the hump with the antiferromagnetic Mott gap feature is compelling. Laughlin[67] clearly showed that the photoemission data evolve with doping to match the SCOC spectrum at half filling. In the Appendix it is shown that the complete doping dependence of the hump is well described by simply doping into the lower Hubbard band of the antiferromagnet.

#### 2. Above $T_c$

In LSCO, the photoemission spectra were observed[66] only in the superconducting state, due to surface degradation at higher temperatures. However, the stripes are clearly better defined in LSCO (the two gap features are more clearly separated) even though $T_c$ is considerably lower, so it is quite possible that the split spectral peaks persist above $T_c$.

In BSCCO, there is a sudden change of the photoemission spectrum at $T_c$: a single broad feature above $T_c$ splits into a peak-dip-hump structure below $T_c$. This is here assumed to be mainly a fluctuation effect: above $T_c$, both features are assumed to be present, but the line broadening is so large that they strongly overlap. Below $T_c$, fluctuations are greatly suppressed, and the linewidth broadening $\Gamma$ is reduced by over an order of magnitude,[71] so the individual spectral features are resolved. Model calculations along these lines have been presented, see Ref. 72 (Fig. 19) and Ref. 73. Superconductivity will also renormalize the gap on the charged stripes, but this is a secondary effect.[72,74]

A long-standing puzzle has been why the Fermi level in optimally-doped BSCCO is so much further from the VHS

(35 meV) than in most other cuprates. However, that estimate[75] was based on the normal-state dispersion, while it is now clear that the appropriate comparison is with the dispersion of the peak feature below $T_c$. In this case, the VHS is estimated to be only 5 meV from the Fermi level.[76]

### C. Summary: Magnetic vs charged pseudogaps

There is a clear progression in the magnetic stripe separation from the Fermi level, from SCOC to LSCO to BSCCO. It is likely that this is due to stripe fluctuation effects, since as more holes fluctuate onto the magnetic stripes the band moves closer to $E_F$ (similar to enhanced charging, Fig. 7). Further evidence for this interpretation lies in the high-$T$ BSCCO spectra, where the peak and hump collapse into a single feature, which continues to resemble the magnetic dispersion (Appendix) and is even closer to $E_F$ than the hump. The conclusion that fluctuations are strongest in BSCCO is consistent with the fact that incommensurate magnetic modulations have not yet been clearly seen in BSCCO.

On the other hand, the charge pseudogap, being fixed by quantum size effects, Eq. (9), is much less sensitive to fluctuations. Results in LSCO and BSCCO are quite similar, and in agreement with the present calculations (Fig. 12). The idea that the pseudogap is associated with stripe minigaps has been proposed previously;[77] the present calculation provides a systematic doping dependence and a connection with the VHS. Since the greatest energy lowering corresponds to having $E_F$ centered on the miniband closest to the VHS (largest DOS, Fig. 15), this is a form of *stripe-induced van Hove splitting*.

The present result improves on an earlier model for the pseudogap.[45] That calculation, based on the photoemission studies of BSCCO in the *normal* state, explained the opening of the pseudogap in terms of a direct crossover from the charged stripe gap to the larger gap on the magnetic stripe. The recent systematic studies in BSCCO (Refs. 68 and 69) and LSCO (Ref. 66) suggest that the low-temperature data are more representative of the stripe phase, and that the pseudogap (or peak feature) is associated with the charged stripes only.

## VI. ISOLATED MAGNETIC STRIPE

Coulomb repulsion inhibits long-range electronic phase separation, resulting in some form of nanoscale phase separation.[34,35] For a two-dimensional charge distribution, the low-energy phases are found to be domain-wall phases, with the minority phase plating out as minimal-width domain walls separating domains of the macroscopic phase.[44] In this situation, there will be a percolation crossover when the minority phase becomes the majority phase.

The present stripe phases share this domain-wall structure, in that the minority phase always appears as minimal width stripes. Strictly speaking, one-dimensional objects do not have a percolation crossover, but at 1/8 doping there is a *duality* crossover, from dominant magnetic to dominant charged stripes, which should be reflected in many properties of the stripes.

For doping less than 1/8, these minimum width charge stripes resemble the domain walls between antiferromagnetic domains proposed in a number of theories;[78] however, for doping greater than 1/8 there are charged domains with magnetic domain walls, a situation not envisaged in these theories.

An important aspect of stripe phase theory is the development of a microscopic model for these domain walls. A number of groups have suggested a connection between magnetic stripes and even-leg ladders. Here, the magnetic domain walls in the higher-doping regime are modeled as two-leg ladders, which develop a spin gap as they move further apart, with reduced interladder coupling.

### A. Spin gap

In a stripe model, the magnetic neutron scattering near $(\pi,\pi)$ should be reflective of the properties of the magnetic stripes. For LSCO, the incommensurability has been discussed above, Fig. 8, and is further discussed in the following subsection. In YBCO, incommensurability has only been resolved at one doping,[8,9] but the doping dependence of the peak width is consistent with a similar underlying, but unresolved incommensurability.[10] In YBCO, the stripe model can also explain the doping dependence of the intensity of the magnetic neutron scattering near $(\pi,\pi)$, as well as the opening of a *spin gap*.

The doping dependence of the net intensity of the magnetic neutron scattering should reflect the relative density of magnetic stripes. For $YBCO_{6+y}$, the intensity was numerically integrated from Fig. 2 of Ref. 79, and the result plotted in Fig. 13. While the relation between $y$ and hole doping $x$ in YBCO is not completely settled, the straight line illustrates a modified Tokura[80] expression, with the doping of the planes starting at $y=0.2$, and varying linearly with $y$. The results are consistent with the picture that all magnetic scattering is associated with the magnetic stripes, and the stripe phase would terminate at an (inaccessible) doping $y=1.095$. This would place the percolation crossover at $y\sim 0.65$, close to the plateau regime. Since the plateau has been interpreted as a 1/8 effect,[81,15] this suggests that the plateau doping is $\sim 0.125$. This fixes the constant of proportionality: $x=0.27(y-0.2)$, so the charged stripe doping, corresponding to $y=1.095$, would be $\sim 0.25$, in excellent agreement with our other estimates. At optimal doping, $y\sim 0.925$, the hole doping would be $\sim 0.2$. These estimates are also consistent with Tokura *et al.*,[80] who found $x=0.125$ for $y=0.75$, $x=0.25$ for $y=1$, and $x=.21$ for optimal doping. The inset to the figure shows that $T_c(x)$ follows the familiar parabolic form[82]

$$\frac{T_c}{T_{c,max}} = 1 - \left(\frac{x-x_m}{x_w}\right)^2, \tag{10}$$

with $T_{c,max}=92$ K, $x_m=0.2$, and $x_w=0.16$. Note that the dip in $T_c$ near the 60-K plateau is close to $x=1/8$. The falloff of intensity is likely to be even steeper than illustrated in Fig. 13, since the data were presented only up to about 60 meV, while at the lower doping levels, there is considerable intensity at higher frequencies.

The spectrum of the excitations near $(\pi,\pi)$ has a complicated evolution with doping, and below the superconducting $T_c$, the intensity is suppressed below a doping dependent energy, called the ''spin gap.''[79] This gap is distinct from the

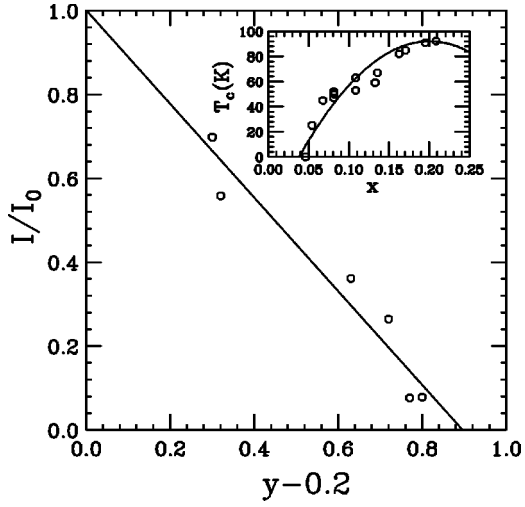


FIG. 13. Intensity of magnetic scattering vs doping for YBCO. Circles=data of Ref. 79; line=expected result for stripe model.

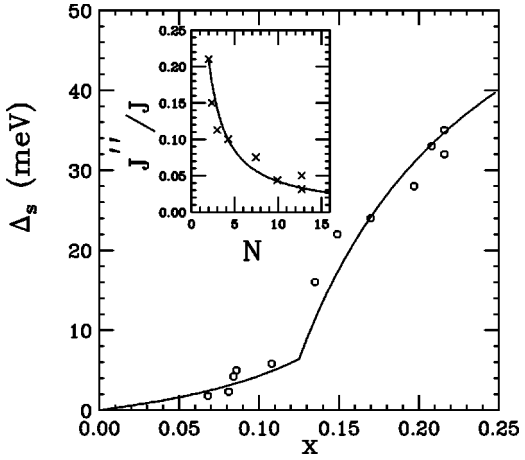


FIG. 14. Spin gap $\Delta_s$ vs doping for YBCO. Circles=data of Ref. 79; line=theory, assuming solid line from inset. Inset: interladder exchange vs hole-doped stripe width.

pseudogap, and has a strikingly different doping dependence (Fig. 14). A similar gap is seen in LSCO,[83,84] but so far only near $x=0.15$. There it is found that the spin gap is isotropic,[84] further evidence that it is distinct from superconductivity or the pseudogap.

The doping dependence of this spin gap in YBCO can be interpreted simply in terms of coupled magnetic ladders (Fig. 14). Below the 1/8 crossover, the magnetic stripe (ladder) width decreases smoothly with doping, while the interladder coupling is approximately constant, since the hole-doped stripe has fixed width. Theoretically, the spin gap is found to be (approximately) inversely proportional to the ladder width,[85] so in this regime the spin gap scales linearly with doping, $\Delta_s=\beta J/M$, where $J$ is the exchange constant, $M$ the ladder width, and $\beta$ a correction for interladder coupling, $\beta \simeq(1-4J''/J)$, with $J''$ the exchange coupling between adjacent ladders.[86] The solid line in Fig. 14 corresponds to $J''=0.21J$.

Above the crossover, $x>x_0/2=0.125$, $M$ is fixed at 2 while $\beta$ increases with doping, since $J''$ decreases as the hole-doped stripes widen. Since the Cu in the hole-doped stripes can be magnetized, the falloff should be relatively slow. Details are model sensitive, but qualitatively the observed behavior is readily reproduced. The curve in Fig. 14 follows from assuming a falloff $J''\sim N^{-1}$, where $N$ is the hole-doped stripe width, inset to Fig. 14. (It should be noted that the falloff is sensitive to the hole-density $x_0$, here taken as 0.25.)

The model predicts[86] that for an isolated stripe, the spin gap equals $J/2$, at least when the exchange constant is the same on all rungs and links. From Fig. 14, this implies a limiting value $J\sim 80$ meV at $x=0.25$, considerably smaller than the $x=0$ value $J=130$ meV. Such a doping dependence for $J$ is not unexpected. For simplicity, however, the model assumes a constant value for $J$; this value must be taken as $J=80$ meV, to successfully model the single stripe limit. The value is less critical near zero doping, where the gap is small.

In this model, the spin gap should already exist in the normal state. The striking change observed at $T_c$ can be explained as a fluctuation effect, similar to those seen in the BSCCO photoemission. Strong fluctuations at high temperatures prevent any long-range stripe order or true spin gap. The superconducting transition leads to three-dimensional coherence, and hence greatly suppresses charge and spin fluctuations in the stripes. Hence a long-range spin gap can open on the magnetic stripes below $T_c$. Consistent with this interpretation, it should be noted that the spectrum in the normal state in heavily doped YBCO has been interpreted[87,84] in terms of a formula derived for spin-1 chains,[88] and hence expected to approximately hold for spin 1/2, two-leg ladders.

One should note the duality between the charge stripe minigap, which grows as hole doping is reduced (Fig. 12), and the magnetic stripe spin gap, which increases with increasing hole doping (Fig. 14).

Two final points should be noted. (i) After the present manuscript was first submitted, Tallon, Loram, and Williams[89] provided considerable additional evidence that the stripe phase terminates at a doping close to $x_0$, and that $T_c$ remains large, even when the stripe phase is absent. (ii) In the regime where magnetic stripes are widely separated, there may be an additional contribution to the magnetic scattering associated with Fermi-surface nesting effects[76] on the charged stripes. It is an outstanding task to combine the two contributions.

### B. Incommensurability saturation

Inelastic magnetic neutron diffraction finds a saturation of the incommensurability in LSCO at approximately $x=1/8$. Within the present framework, there are actually several possible explanations for the saturation. One was discussed above (Fig. 8): strong Coulomb interactions arrest the phase separation at the (2,2) stripe, and higher doping causes these stripes to gradually fill in.

On this interpretation, the Coulomb effects are much stronger in LSCO than in YBCO, and the isolated spin gap regime (right-hand side of Fig. 14) would not exist in LSCO. The Coulomb effects would indeed be expected to be stronger in LSCO, since interlayer screening is weaker. In Nd-substituted LSCO, due to the low-temperature tetragonal (LTT) phase structural distortions, stripes in alternate layers

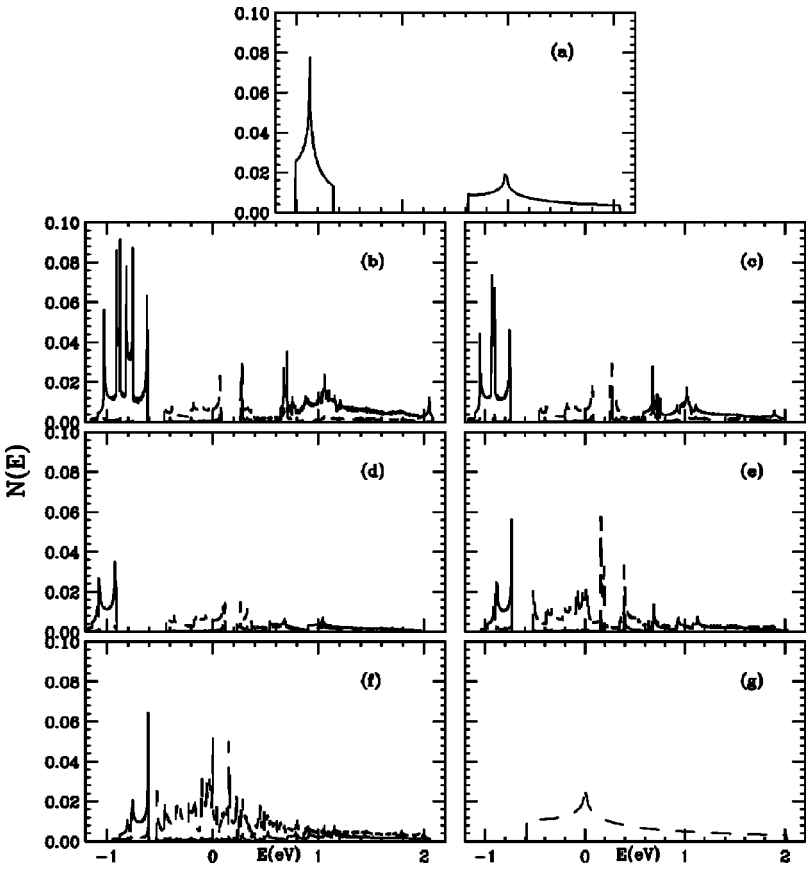


FIG. 15. Density of states for dopings: $x = 0$ (a), 0.0625 (b), 0.0833 (c), 0.125 (d), 0.167 (e), 0.1875 (f), and 0.25 (g) assuming dielectric constant $\epsilon = 15$. (The $x = 0$ data are shifted up by 0.16 eV.) Solid (dashed) line=partial density of states for magnetic (charged) stripes.

are rotated by 90°; a similar situation may arise in LSCO, perhaps due to LTT fluctuations. On the other hand, in YBCO the magnetic correlations have a strong *c*-axis modulation, suggesting that stripes in both $CuO_2$ planes of a bilayer run parallel, with the charged stripes offset laterally to provide stronger interlayer screening.

However, there are other plausible explanations for incommensurability saturation. Even before the discovery of stripes, it was found that low-temperature orthorhombic (LTO) and LTT domains of fairly large size (producing distinguishable diffraction peaks) coexist near 1/8 doping in LBCO. It seems plausible that this is associated with a stripe commensurability effect, similar to that found in the nickelates, and that a similar effect arises, at least incipiently in LSCO. In this case, the residual magnetic scattering would be due to regions that have not yet been doped beyond 1/8. In the more highly doped domains, the magnetic stripes would have a spin gap: since the ground state of a two-leg ladder is a spin singlet, it does not contribute to the magnetic scattering. A related problem has been studied by Kim *et al.*,[90] who showed that in a random mix of weakly coupled three-leg (magnetic) ladders and two-legged (spin-gapped, and hence nonmagnetic) ladders, the magnetic incommensurability remains unchanged from that of the pure array of three-legged ladders.

Even without commensurability effects, one would expect 1/8 lock-in over a finite doping range, when the 2,2 stripes coexist with 2,4 stripes, which have a well defined spin gap. In this case, the magnetic incommensurability should be fixed at that for 1/8 throughout the coexistence regime, but should disappear when a commensurate 2,4 phase is stable, at $x = 2x_0/3 \simeq 0.17$. In LSCO, the 1/8 stripes are actually found[1,2] to persist up to $x \simeq 0.25$. Hence the need to postulate lock-in effects at 1/8 doping, the exact analog of the stability of the $x = 1/3$ and 1/2 striped phases in nickelates. In this case, the heavily doped phases would have no magnetic scattering, while the 1/8 stripes would have a scattering of fixed incommensurability, but decreasing intensity and increasing width, as the stripe domains shrink in size. The special stability of the 1/8 phase may be associated with the finite residual exchange coupling across the two-cell-wide charged stripes, which is responsible for the antiphase boundaries, and which may be lost in wider charged stripes, or with the reduced Coulomb energy.

At this stage, there is not enough information to judge between the two models for incommensurability saturation. The former, strong Coulomb effect, has the advantage that it could simultaneously explain why $T_c$ in LSCO is so low—the local hole density is forced away from optimal. However, there is considerable evidence that stripe phase order is better developed in LSCO than in other cuprates, and this could provide reason enough for a lower $T_c$.

In many ways, optimally doped LSCO resembles an underdoped YBCO. We have here suggested that this is because stripes and pseudogaps in both materials persist up to $x \simeq 0.25$, whereas $T_c$ is optimal near 0.16 in LSCO, 0.2 in YBCO. Sato *et al.*[91] have recently provided additional evidence that the pseudogap opens well above $T_c$ in optimally doped LSCO.

## VII. DISCUSSION

### A. Improvements for the stripe model

The present model provides a significant advance in the understanding of the stripe phase. Earlier calculations[20,21] found that the stripes produce minigaps, but that an average, smeared dispersion and Fermi surface could still be defined. The present calculation studies how holes redistribute in the presence of a competition between a doping dependent chemical potential, which favors phase separation, and Coulomb repulsion, which favors a uniform density distribution. The full doping dependence of the dispersion is calculated, with the striking result that the resulting dispersion resembles a weighted superposition of the dispersions of the two end phases, with the addition of some superlattice minigaps. This is very encouraging, in providing an explanation for the photoemission results. Moreover, it shows that the mechanisms responsible for the special stability of the end phases can continue to operate on these nanoscopic length scales.

A number of improvements still need to be made in the model. The next step would be to make the calculation fully self-consistent, deriving the chemical potential by directly calculating and minimizing the free energy of the striped phase. Since the dispersion is not greatly changed, it is unlikely that this additional step will greatly modify the present results. The most likely change would be that the densities could adjust slightly to take advantage of the minigaps, better centering them at the Fermi level. This could lead to a more systematic growth of the pseudogap with underdoping, since the minigaps are associated with the charged stripes, and get larger as these stripes get narrower.

A complete understanding of the stripe phase, particularly in BSCCO, lies in the correct inclusion of fluctuation effects. These effects can broadly be separated into two categories, depending on whether the fluctuation preserves the local density distribution or not. In the former category fall fluctuations in the local stripe spacing, either static or slowly varying in time, and long-wavelength bending of the stripes. It is likely that the energy dispersion is a fairly localized function in space, and that these fluctuations can be calculated as weighted averages over the present solutions. In this case, the dispersion would still be a superposition of the two end phases, and the main effect of the fluctuations would be to smear out the minigaps. Since there is always a gap near the Fermi level, a residual pseudogap should survive. Moreover, since the split-off LHB is well defined, particularly at lower doping, it should persist as a distinguishable feature after averaging. This would resemble the photoemission in LSCO.

The second class of fluctuations involves fluctuations which are fast enough, or disordered on a sufficiently short-wavelength scale so that the local density does not lie near the two potential minima. These fluctuations act to wipe out the stripe fluctuations on a local level, and the question is, can they describe the experimental results in BSCCO, where, for $T>T_c$, the two valence bands appear to collapse into a single reconstructed band. This is a plausible result: as a line of holes fluctuates back and forth in an antiferromagnetic background, the background will have to adjust to some time-averaged hole density. The theoretical problem is how to properly include this averaging: it is a question of how the system responds locally on different time scales.

### B. Density of states

Figure 15 shows the calculated densities of states for a number of stripe configurations, illustrating how the charged stripes gradually fill in the Mott-Hubbard gap. Within the charged stripe dispersion, there is a single prominent minigap, shown on expanded scale in Fig. 16, close to half filling of the charged stripe, which gradually closes up with increased doping. Comparison with Fig. 7 shows that this is the minigap closest to the VHS. Doping of the charged stripe moves the Fermi level into the miniband below this gap, approximately centered between two flat band states.

### C. Fermi surface and remnant Fermi surface

Figure 17 shows the Fermi surfaces corresponding to the same dopings as in Fig. 7. As expected from the ''projected'' dispersions in that figure, in all cases the wave functions are $>90\%$ associated with the charged stripes. Note the important role of the structure factors: while there is a well-defined superlattice in each case, and hence each Fermi-surface segment is periodically repeated, the weight is highly nonuniformly distributed, being concentrated predominantly near the limiting $x=0.25$ Fermi surface (solid line in the figures).

The large flat sections of the 1/8 stripe pattern, Fig. 17(b) may have been seen experimentally, both in Nd-substituted LSCO at the 1/8 anomaly[92] and in BSCCO,[93] although the latter result is disputed.[94]

Ronning *et al.*[57] introduced an alternative, well-defined energy surface, which they refer to as a ''remnant Fermi surface'' (rFs). This is the locus of points where the integrated photoemission intensity, taken as proportional to $n(k)$, falls to one half its maximal value. While the intensity does fall to half at the Fermi level, it can also fall to half at an energy away from the Fermi level (N.B., the rFs is not a surface of constant energy). Indeed, a rFs was found for the insulating $Ca_2CuO_2Cl_2$. We have shown[95] that in this case the rFs (the locus of points where the coherence factor equals one-half) maps out the superlattice zone boundary. (Since the model does not include fluctuations, there is only one band below $E_F$, and hence no photoemission distribution to integrate over.)

In the case of a stripe array, there are several complications. First, there are several subbands, and one will get different results depending on whether one calculates an rFs for each subband, or a single rFs for the whole valence band. The structure factor provides an additional complication, since the intensity is almost never the full possible value. Nevertheless, for simplicity, Fig. 18 plots the locus of points where the net spectral function equals 1/2—actually, falls within a range 0.48–0.52. Comparison of Fig. 17 and 18 shows that the true Fermi surface and the rFs are quite distinct features, and that the rFs tends to follow the superlattice Brillouin-zone boundaries.

### D. QCP's?

While there have been a number of suggestions that a quantum critical point (QCP) exists in the cuprates,[96] the

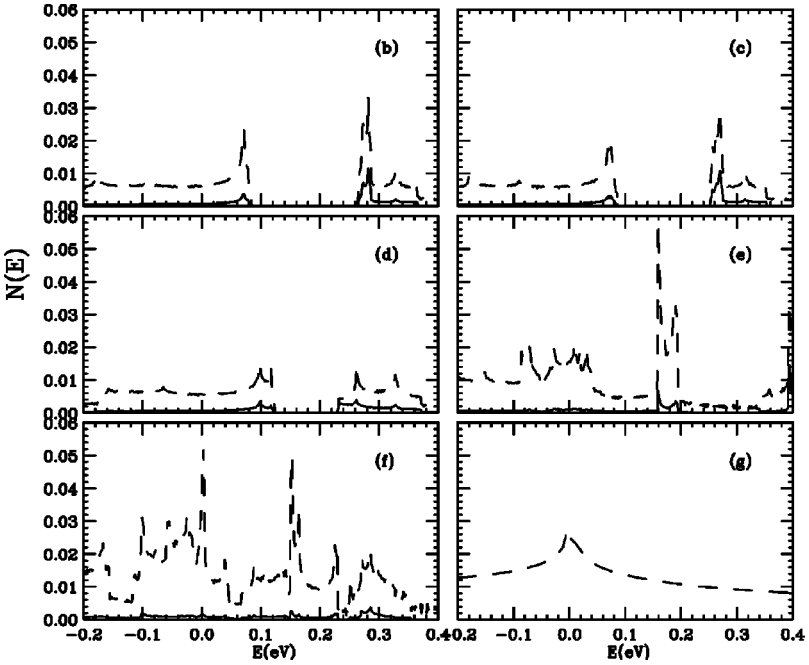


FIG. 16. Blowup of density of states near $E_F$, for same dopings as in Fig. 15. (There is no frame (a), since the DOS vanishes in this energy regime.)

present model suggests rather a series of preferred dopings corresponding to commensurate stripes—much as found in the nickelates. The most prominent special dopings are the 1/8 anomaly, corresponding to the duality crossover from magnetic-dominated to charge-dominated stripes, and the termination of the stripe phases,[89] at approximately twice that density, $x_0 \simeq 0.25$. However, there are hints that other special dopings also play a role. Thus the high-field localization transition in LSCO (Ref. 97) occurs at $x=0.17$, close to the first appearance of two-leg-wide charged stripes at $x=2x_c/3 \simeq 0.167$. Again, the superconducting transition terminates (and the horizontal-vertical stripes are replaced by diagonal stripes)[28] at $x=0.058$, close to the doping $x_0/4$ where the charged stripes first separate by more than four magnetic cells.

### E. Comparisons with slave boson results

It is instructive to compare the present results with earlier slave boson calculations. In the simplest version, there is no magnetic coupling, $J=0$, and the band structure near the Mott transition is highly anomalous. There is a single band, but as the doping approaches half filling, $x \to 0^+$, the bandwidth vanishes, with both $t$ and $t'$ renormalized to zero. In the three-band model, even after setting $U \to \infty$, there is still a charge transfer energy, $\Delta$. In this case, it is also possible to approach half filling from below, $x \to 0^-$; the same bandwidth collapse occurs, but at a different energy, $E^-$, with $E^- - E^+$ being the (renormalized) charge transfer energy.

Is there any way to reconcile the present results with slave boson theory? I suggest the following possibility. When a hole is doped into the Mott insulator, there is phase separation, and locally the dispersion is restored: $t \to t_0$. At a doping $x$, a fraction $x/x_0$ of the electrons have hopping $\sim t$, the rest $\sim 0$. But in the mean-field slave boson calculation the effect of the hole is uniformly spread out over the entire lattice, leading to an effective $t \to x t_0$. This is just what is found in the present stripe calculation. As the material is doped, the magnetic band persists with little change, while a new band appears, characteristic of the hole-doped stripes, with full bandwidth, $t \sim t_0$ (neglecting superlattice gaps), but with relative intensity proportional to $x$, (Fig. 7). If this interpretation is correct, it suggests that the slave boson calculation may underestimate the tendency for phase separation.

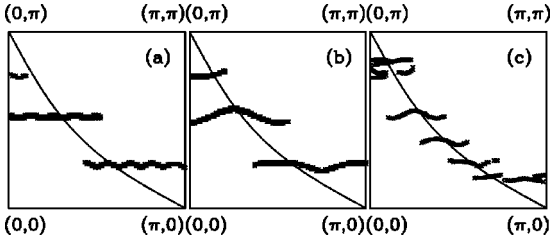


FIG. 17. Fermi surfaces for dopings: $x=$ 0.0625 (a), 0.125 (b), and 0.1875 (c), and $\epsilon=15$. Solid line in each is the Fermi surface for $x=0.25$.

## VIII. CONCLUSIONS

This has been a long manuscript, which presents a coherent view of the stripe phases in the cuprates. A number of principal results of the calculations are here summarized. Most of the results are *generic*, and would be expected in any model where the stripes result from two-phase coexistence, while a few are specific to a van Hove scenario.

(i) The stripes arise from a frustrated phase separation, i.e., there are two preferred hole dopings with independent dispersions, one characteristic of antiferromagnetism.

(ii) This allows a study of the evolution of the dispersion as a function of hole doping.

(iii) It is found that, even at this nanoscale level, the dispersion can be characterized as a *superposition of two components*, leading to a picture of magnetic stripe bands and hole-doped (''charged'') stripe bands. This allows a natural interpretation of the photoemission spectra in LSCO, and suggests a unified picture with BSCCO and SCOC.

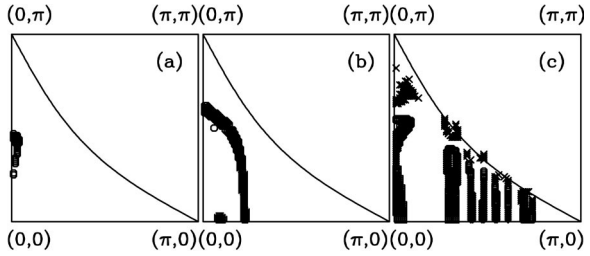


FIG. 18. Remnant Fermi surfaces for same dopings as in Fig. 17: $x = 0.0625$ (a), 0.125 (b), and 0.1875 (c).

(iv) The calculations suggest that an important role of the superconducting transition is to freeze out fluctuations of the stripes. This freezeout manifests itself in three ways: (a) the electron-electron scattering rate drops by several orders of magnitude below $T_c$;[71] (b) the photoemission dispersion splits in BSCCO into a characteristic peak-dip-hump structure; (c) the $(\pi,\pi)$ magnetic neutron scattering in YBCO sharpens below $T_c$, revealing a characteristic spin gap.

(v) The doping dependence naturally leads to a picture of a series of *quantum critical points* (QCP's) or magic dopings, at which the stripe pattern is commensurate with the crystalline lattice. The most prominent one is the famous 1/8 effect, but the metal-insulator transition in LSCO and the onset of superconductivity are close to two other magic numbers.

(vi) The percolation crossover at 1/8 doping provides a simple model of the spin gap in YBCO, showing that a two-leg ladder provides a good model for an isolated magnetic stripe.

(vii) As a result of point (iii), the model has a *natural VHS pinning* to the Fermi level: if the VHS is at the Fermi level in the charged stripe end phase (as it must be, if this phase is stabilized by van Hove nesting), then the VHS remains close to $E_F$ over the entire doping range.

(viii) This provides a new explanation of the pseudogap: *stripe-induced Van Hove splitting*.

(ix) More speculatively, since superconductivity in YBCO is strongest well beyond the percolation crossover (1/8 effect), *superconductivity seems to be a property predominantly of the charged stripes*. The recent data of Tallon, Loram, and Williams[89] strengthen this possibility.

There are a number of advantages of the present model of fractionally doped stripes. First, if the stripes are stabilized by CDW formation, then there is an important continuity between stripes in the cuprates, and those in the nickelates and manganites. Such continuity is lost in the $SO(5)$ model, where the charged stripes are stabilized by superconductivity. Moreover, a connection with CDW's would naturally explain the experimental observation that the stripe phases are dominated by charge order rather than spin order, a result difficult to understand in a pure Hubbard or $tJ$ model.

*Note added in proof.* Section VI B: Recent work by Büchner *et al.*[99] suggests that in RE-substituted LSCO there is phase separation between $\frac{1}{8}$-anomaly domains ($x=0.125$) and fully doped domains ($x=0.25$). Thus ''bulk superconductivity'' is found only for $x>0.18$, close to the percolation crossover $(0.125+0.25)/2$.

Section VII E: Orenstein and Millis[100] recently posed the Lee-Wen paradox:[101] Lee and Wen showed that they could explain the Uemura relation for underdoped cuprates in terms of flux phase physics, as long as the flux phase dispersion is independent of doping. The paradox is that many strong-coupling models expect the dispersion to renormalize to zero near the Mott insulator at half filling. As discussed in Sec. VII E, for stripes this renormalization is taken as indicating that the *fraction of material* associated with charged stripes renormalizes to zero at half filling, whereas *the dispersion on a single stripe* is less sensitive to doping. Thus, the paradox is explained if the flux phase exists on the charged stripes. Indeed, the flux phase is a form of dynamic charge-density wave, closely related to the CDW and LTT phases,[102] and hence could well live on charged stripes.

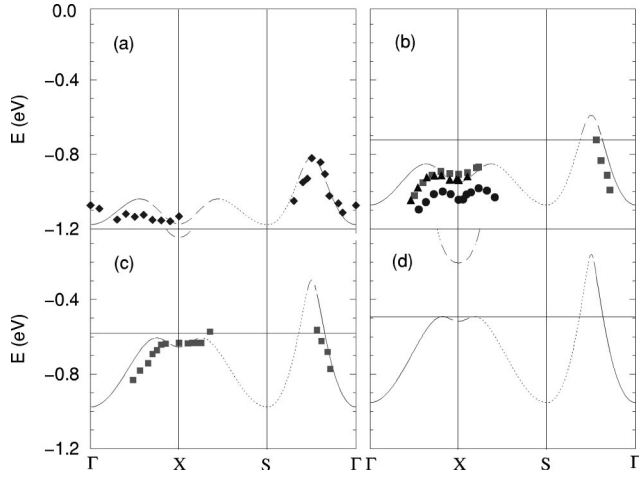


FIG. 19. Dispersion of the doped antiferromagnet in mean-field model, for $x=0$ (a), 0.169 (b), 0.356 (c), and 0.392 (d). Data of Ref. 56=diamonds (SCOC); Ref. 98=squares [BSCCO (b) underdoped, $T_c=67$ K; (c) overdoped, $T_c=85$ K]; and Ref. 68: BSCCO, triangles (underdoped, $T_c=52$ K) and circles (overdoped, $T_c=72$ K). Solid lines: coherence factor $>0.8$; dashed lines: $0.8>$coherence factor$>0.2$; dotted lines: coherence factor $<0.2$. Horizontal lines=Fermi level.

## ACKNOWLEDGMENTS

These computations were carried out using the facilities of the Advanced Scientific Computation Center at Northeastern University (NU-ASCC). Their support is gratefully acknowledged. I thank C. Kusko, S. Sridhar, A. Bansil, B. Barbellini, and M. Lindros for stimulating conversations. This is publication 776 of the Barnett Institute.

## APPENDIX: MORE ON THE SDW DISPERSION

The SDW model, Sec. III A, gives a good description of the magnetic photoemission dispersion for insulating SCOC, for the hump feature in superconducting BSCCO, and for normal-state BSCCO (Fig. 19). For all curves, the band parameters given below Eq. (4), are used, with $M(x)$ found self-consistently. The spectral weight is proportional to the coherence factor

$$\zeta_{\pm}=\frac{1}{2}\left(1\pm\frac{\epsilon_{-}}{W}\right), \tag{A1}$$

with the subscript + (−) referring to the upper (lower) Hubbard band.

The results are qualitatively consistent with the insulating oxyclorides[56,57] and both the hump pseudogap (diamonds and squares),[68] and the normal-state pseudogap (×) (Refs. 98 and 68) in BSCCO. The fact that the normal-state pseudogap has the dispersion of the lower Hubbard band has been noted by a number of groups, including Schmalian, Pines, and Stojkovic,[53] and Misra *et al.*[54] Note that the self-consistent hole dopings are quite large, and are very different for the hump and normal-state features. As discussed in Sec. V, the shift of the lower Hubbard band is presumably due to fluctuation-induced hole filling of the magnetic stripes.

The first-order transition to the paramagnetic phase evident in Fig. 1 is a topological transition, arising when the Fermi level crosses the band dispersion near $X$ [Fig. (19)d]. This is rather striking, since topological transitions are typically rather weak—of order 2.5. A similar result was found in the Hubbard model ($t'=0$) by Guinea *et al.*[55]


[1] J.M. Tranquada, B.J. Sternlieb, J.D. Axe, Y. Nakamura, and S. Uchida, Nature (London) **375**, 561 (1995); J.M. Tranquada, J.D. Axe, N. Ichikawa, A.R. Moodenbaugh, Y. Nakamura, and S. Uchida, Phys. Rev. Lett. **78**, 338 (1997).

[2] K. Yamada, C.H. Lee, K. Kurahashi, J. Wada, S. Wakimoto, S. Ueki, H. Kimura, Y. Endoh, S. Hosoya, G. Shirane, R.J. Birgeneau, M. Greven, M.A. Kastner, and Y.J. Kim, Phys. Rev. B **57**, 6165 (1998).

[3] T. Suzuki, T. Goto, K. Chiba, T. Shinoda, T. Fukase, H. Kimura, K. Yamada, M. Ohashi, and Y. Yamaguchi, Phys. Rev. B **57**, 3229 (1998); H. Kimura, K. Hirota, H. Matsushita, K. Yamada, Y. Endoh, S.-H. Lee, C.F. Majkrzak, R. Erwin, G. Shirane, M. Greven, Y.S. Lee, M.A. Kastner, and R.J. Birgeneau, *ibid.* **59**, 6517 (1999).

[4] S. Wakimoto, G. Shirane, Y. Endoh, K. Hirota, S. Ueki, K. Yamada, R.J. Birgeneau, M.A. Kastner, Y.S. Lee, P.M. Gehring, and S.H. Lee, Phys. Rev. B **60**, 769 (1999); S. Wakimoto, K. Yamada, S. Ueki, G. Shirane, Y.S. Lee, S.H. Lee, M.A. Kastner, K. Hirota, P.M. Gehring, Y. Endoh, and R.J. Birgeneau, J. Phys. Chem. Solids **60**, 1079 (1999).

[5] Y.S. Lee, R.J. Birgeneau, M.A. Kastner, Y. Endoh, S. Wakimoto, K. Yamada, R.W. Erwin, S.H. Lee, and G. Shirane, Phys. Rev. B **60**, 3643 (1999).

[6] A.W. Hunt, P.M. Singer, K.R. Thurber, and T. Imai, Phys. Rev. Lett. **82**, 4300 (1999).

[7] M.-H. Julien, F. Borsa, P. Carretta, M. Horvatić, C. Berthier, and C.T. Lin, Phys. Rev. Lett. **83**, 604 (1999).

[8] P. Dai, H.A. Mook, and F. Dogan, Phys. Rev. Lett. **80**, 1738 (1998); H.A. Mook, P. Dai, S.M. Hayden, G. Aeppli, T.G. Perring, and F. Dogan, Nature (London) **395**, 580 (1998).

[9] M. Arai, T. Nishijima, Y. Endoh, T. Egami, S. Tajima, K. Tomimoto, Y. Shiohara, M. Takahashi, A. Garrett, and S.M. Bennington, Phys. Rev. Lett. **83**, 608 (1999).

[10] A.V. Balatsky and P. Bourges, Phys. Rev. Lett. **82**, 5337 (1999).

[11] H.L. Edwards, A.L. Barr, J.T. Markert, and A.L. de Lozanne, Phys. Rev. Lett. **73**, 1154 (1994).

[12] H.A. Mook, F. Dogan, and B.C. Chakoumakos, cond-mat/9811100, J. Supercond. (to be published); H.A. Mook and B.C. Chakoumakos, J. Supercond. **10**, 389 (1997).

[13] R.J. McQueeney, Y. Petrov, T. Egami, M. Yethiraj, G. Shirane, and Y. Endoh, Phys. Rev. Lett. **82**, 628 (1999).

[14] H.A. Mook (unpublished); M. Gutmann, S.J.L. Billinge, E.L. Brosha, and G.H. Kwei, Phys. Rev. B **61**, 11 762 (2000).

[15] M. Akoshima, T. Noji, Y. Ono, and Y. Koike, Phys. Rev. B **57**, 7491 (1998).

[16] N. Saini, J. Avila, A. Bianconi, A. Lanzara, M.C. Ascensio, S. Tajima, G.D. Gu, and N. Koshizuka, Phys. Rev. Lett. **79**, 3467 (1997).

[17] Z.-X. Shen, P.J. White, D.L. Feng, C. Kim, G.D. Gu, H. Ikeda, R. Yoshizaki, and N. Koshizuka, Science **280**, 259 (1998).

[18] J. Mesot, M.R. Norman, H. Ding, and J.C. Campuzano, Phys. Rev. Lett. **82**, 2618 (1999); J.C. Campuzano, H. Ding, H. Fretwell, J. Mesot, A. Kaminski, T. Yokoya, T. Takahashi, T. Mochiku, and K. Kadowaki, cond-mat/9811349 (unpublished).

[19] P.J. White, Z.-X. Shen, D.L. Feng, C. Kim, M.-Z. Hasan, J.M. Harris, A.G. Loeser, H. Ikeda, R. Yoshizaki, G.D. Gu, and N. Koshizuka, cond-mat/9901349 (unpublished).

[20] M.I. Salkola, V.J. Emery, and S.A. Kivelson, Phys. Rev. Lett. **77**, 155 (1996).

[21] G. Seibold, F. Becca, F. Bucci, C. Castellani, C. di Castro, and M. Grilli, cond-mat/9906108 (unpublished).

[22] D. Poilblanc and T.M. Rice, Phys. Rev. B **39**, 9749 (1989); H. Schulz, J. Phys. (Paris) **50**, 2833 (1989); J. Zaanen and O. Gunnarsson, Phys. Rev. B **40**, 7391 (1989); M. Inui and P.B. Littlewood, Phys. Rev. B **44**, 4415 (1991).

[23] J.A. Vergés, E. Louis, M.P. López-Sancho, F. Guinea, and A.R. Bishop, Phys. Rev. B **43**, 6099 (1991).

[24] K. Yonemitsu, A.R. Bishop, and J. Lorenzana, Phys. Rev. B **47**, 8065 (1993); **47**, 12 059 (1993).

[25] B. Valenzuela, M. Vozmediano, and F. Guinea, cond-mat/9909224 (unpublished).

[26] G. Seibold, E. Sigmund, and V. Hizhnyakov, Phys. Rev. B **57**, 6937 (1998).

[27] For nickelates, see S.H. Lee and S.-W. Cheong, Phys. Rev. Lett. **79**, 2514 (1997).

[28] S. Wakimoto, G. Shirane, Y. Endoh, K. Hirota, S. Ueki, K. Yamada, R.J. Birgeneau, M.A. Kastner, Y.S. Lee, P.M. Gehring, and S.H. Lee, Phys. Rev. B **60**, 769 (1999); S. Wakimoto, R.J. Birgeneau, M.A. Kastner, Y.S. Lee, R. Erwin, P.M. Gehring, S.H. Lee, M. Fujita, K. Yamada, Y. Endoh, K. Hirota, and G. Shirane, Phys. Rev. B **61**, 3699 (2000).

[29] C.H. Chen, S.-W. Cheong, and A.S. Cooper, Phys. Rev. Lett. **71**, 2461 (1993); S.-W. Cheong, H.Y. Hwang, C.H. Chen, B. Batlogg, L.W. Rupp, Jr., and S.A. Carter, Phys. Rev. B **49**, 7088 (1994).

[30] S. Mori, C.H. Chen, and S.-W. Cheong, Nature (London) **392**, 473 (1998).

[31] T. Mutou and H. Kontani, Phys. Rev. Lett. **83**, 3685 (1999).

[32] X.X. Bi and P.C. Ecklund, Phys. Rev. Lett. **70**, 2625 (1993).

[33] J. Zaanen and A.M. Oles, Ann. Phys. (Leipzig) **5**, 224 (1996).

[34] P.B. Visscher, Phys. Rev. B **10**, 943 (1974).

[35] E.L. Nagaev, *Physics of Magnetic Semiconductors* (Mir, Moscow, 1983).

[36] C. Nayak and F. Wilczek, Phys. Rev. Lett. **78**, 2465 (1997).
[37] V.J. Emery, and S.A. Kivelson, Physica C **209**, 597 (1993).
[38] A. Auerbach and B.E. Larson, Phys. Rev. Lett. **66**, 2262 (1991).
[39] S.R. White and D.J. Scalapino, Phys. Rev. Lett. **80**, 1272 (1998).
[40] S.R. White and D.J. Scalapino, Phys. Rev. Lett. **81**, 3227 (1998).
[41] R. Hlubina, S. Sorella, and F. Guinea, Phys. Rev. Lett. **78**, 1343 (1997); R. Hlubina, Phys. Rev. B **59**, 9600 (1999).
[42] H.J. Schulz, Phys. Rev. B **39**, 2940 (1989).
[43] R.S. Markiewicz and M.T. Vaughn, J. Phys. Chem. Solids **59**, 1737 (1998); Phys. Rev. B **57**, 14 052 (1998).
[44] R.S. Markiewicz, J. Phys.: Condens. Matter **2**, 665 (1990).
[45] R.S. Markiewicz, Phys. Rev. B **56**, 9091 (1997).
[46] H.-H. Lin, L. Balents, and M.P.A. Fisher, Phys. Rev. B **58**, 1794 (1998).
[47] R.S. Markiewicz, C. Kusko, and M.T. Vaughn, cond-mat/9807067, J. Supercond. (to be published).
[48] H. Tsunetsugu, M. Troyer, and T.M. Rice, Phys. Rev. B **51**, 16 456 (1995).
[49] J.R. Schrieffer, X.G. Wen, and S.C. Zhang, Phys. Rev. B **39**, 11 663 (1989).
[50] A. Kampf and J. Schrieffer, Phys. Rev. B **41**, 6399 (1990).
[51] N. Bulut, D.J. Scalapino, and S.R. White, Phys. Rev. Lett. **73**, 748 (1994).
[52] A.V. Chubukov and D.K. Morr, Phys. Rev. B **57**, 5298 (1998).
[53] J. Schmalian, D. Pines, and B. Stojković, Phys. Rev. Lett. **80**, 3839 (1998).
[54] S. Misra, R. Gatt, T. Schmauder, A.V. Chubukov, M. Onellion, M. Zacchigna, I. Vobornik, F. Zwick, M. Grioni, G. Margaritondo, C. Quitmann, and C. Kendziora, Phys. Rev. B **58**, 8905 (1998).
[55] F. Guinea, E. Louis, M.P. López-Sancho, and J.A. Vergés, Solid State Commun. **113**, 593 (2000).
[56] B.O. Wells, Z.X. Shen, A. Matsuura, D.M. King, M.A. Kastner, M. Greven, and R.J. Birgeneau, Phys. Rev. Lett. **74**, 964 (1995).
[57] C. Kim, P.J. White, Z.-X. Shen, T. Tohyama, Y. Shibata, S. Maekawa, B.O. Wells, Y.J. Kim, R.J. Birgeneau, and M.A. Kastner, Phys. Rev. Lett. **80**, 4245 (1998); F. Ronning, C. Kim, D.L. Feng, D.S. Marshall, A.G. Loesser, L.L. Miller, J.N. Eckstein, I. Bozovic, and Z.-X. Shen, Science **282**, 2067 (1998).
[58] J.W. Loram, K.A. Mirza, J.R. Cooper, N.A. Thanassopoulou, and W.Y. Liang, in *Proceedings of the 10th Anniversary HTS Workshop on Physics, Materials, and Applications*, edited by B. Batlogg, C.W. Chu, D.U. Gubser, and K.A. Müller (World Scientific, Singapore, 1996), p. 341; see discussion on pp. 1203–4 of Ref. 60.
[59] R.S. Markiewicz, J. Phys. Chem. Solids **58**, 1179 (1997).
[60] K. Dichtel, R.J. Jelitto, and H. Koppe, Z. Phys. **251**, 173 (1972).
[61] H. Eskes and A.M. Oleś, Phys. Rev. Lett. **73**, 1279 (1994).
[62] S. Uchida, T. Ido, H. Takagi, T. Arima, Y. Tokura, and S. Tajima, Phys. Rev. B **43**, 7942 (1991).
[63] R.S. Markiewicz and M.T. Vaughn, in *High Temperature Superconductivity*, edited by S.E. Barnes, J. Ashkenazi, J.L. Cohn, and F. Zuo (AIP, Woodbury, NY, 1999), p. 75 [correct Fig. 2 available at cond-mat/9903422 (unpublished)].
[64] M. Veillette, Ya.B. Bazaliy, A.J. Berlinsky, and C. Kallin, Phys. Rev. Lett. **83**, 2413 (1999).
[65] J. Humlicek, A.P. Litvinchuk, W. Cress, B. Lederle, C. Thomsen, M. Cardona, H.L. Habermeier, I.E. Trofimov, and W. Konig, Physica C **206**, 345 (1993).
[66] A. Ino, C. Kim, M. Nakamura, T. Mizokawa, Z.-X. Shen, A. Fujimori, T. Kakeshita, H. Eisaki, and S. Uchida, cond-mat/9902048, Phys. Rev. B (to be published).
[67] R.B. Laughlin, Phys. Rev. Lett. **79**, 1726 (1997).
[68] J.C. Campuzano, H. Ding, M.R. Norman, H.M. Fretwell, M. Randeria, A. Kaminski, J. Mesot, T. Takeuchi, T. Sato, T. Yokoya, T. Takahashi, T. Mochiku, K. Kadowaki, P. Guptasarma, D.G. Hinks, Z. Konstantinovic, Z.Z. Li, and H. Raffy, Phys Rev. Lett. **83**, 3709 (1999).
[69] J.F. Zasadzinski, Bull. Am. Phys. Soc. **44**, 1503 (1999).
[70] A. Kaminski, J. Mesot, H. Fretwell, J.C. Campuzano, M.R. Norman, M. Randeria, H. Ding, T. Sato, T. Takahashi, T. Mochiku, K. Kadowaki, and H. Hoechst, Phys. Rev. Lett. **84**, 1788 (2000).
[71] D.A. Bonn, P. Dosanjh, R. Liang, and W.L. Hardy, Phys. Rev. Lett. **68**, 2390 (1992); K. Krishana, J.M. Harris, and N.P. Ong, *ibid.* **75**, 3529 (1995); M.R. Norman, M. Randeria, H. Ding, and J.C. Campuzano, Phys. Rev. B **57**, 11 093 (1998).
[72] R.S. Markiewicz, C. Kusko, and V. Kidambi, Phys. Rev. B **60**, 627 (1999).
[73] A.V. Chubukov and D.K. Morr, Phys. Rev. Lett. **81**, 4716 (1998).
[74] R.S. Markiewicz and C. Kusko, cond-mat/9810214 (unpublished).
[75] M.R. Norman, M. Randeria, H. Ding, and J.C. Campuzano, Phys. Rev. B **52**, 615 (1995).
[76] M.R. Norman, cond-mat/9912203 (unpublished).
[77] A. Bianconi, A. Valletta, A. Perali, and N.L. Saini, Physica C **296**, 269 (1998); C.C. Tsuei and T. Doderer, Eur. Phys. J. B **10**, 257 (1999).
[78] R.B. Laughlin, cond-mat/9709195 (unpublished); J. Zaanen, J. Phys. Chem. Solids **59**, 1769 (1998).
[79] P. Bourges, L.P. Regnault, J.Y. Henry, C. Vettier, Y. Sidis, and P. Burlet, Physica B **215**, 30 (1995).
[80] Y. Tokura, J.B. Torrance, T.C. Huang, and A.I. Nazzal, Phys. Rev. B **38**, 7156 (1988).
[81] J.L. Tallon, in *Proceedings of the 10th Anniversary HTS Workshop on Physics, Materials, and Applications* (Ref. 58), p. 292.
[82] J.L. Tallon, C. Bernhard, H. Shaked, R.L. Hitterman, and J.D. Jorgensen, Phys. Rev. B **51**, 12 911 (1995).
[83] K. Yamada, S. Wakimoto, G. Shirane, C.H. Lee, M.A. Kastner, S. Hosoya, M. Greven, Y. Endoh, and R.J. Birgeneau, Phys. Rev. Lett. **75**, 1626 (1995); S. Petit, A.H. Moudden, B. Hennion, A. Vietkin, and A. Revcolevchi, Physica B **234-236**, 800 (1997).
[84] B. Lake, G. Aeppli, T.E. Mason, A. Schröder, D.F. McMorrow, K. Lefmann, M. Isshiki, M. Nohara, H. Takagi, and S.M. Hayden, Nature (London) **400**, 43 (1999).
[85] E. Dagotto and T.M. Rice, Science **271**, 618 (1996).
[86] S. Gopalan, T.M. Rice, and M. Sigrist, Phys. Rev. B **49**, 8901 (1994).
[87] P. Bourges, in *Gap Symmetry and Fluctuations in High Temperature Superconductors*, edited by J. Bok, G. Deutscher, D. Pavuna, and S.A. Wolf (Plenum, New York, 1998).
[88] L.P. Regnault, I. Zaliznyak, J.P. Renard, and C. Vettier, Phys. Rev. B **50**, 9174 (1994).
[89] J.L. Tallon, cond-mat/9911422 [Advances in Supercond. XII (Springer, Tokyo, in press); J.L. Tallon, J.W. Loram, and G.V.M. Williams, cond-mat/9911423, Physica C (to be published).
[90] Y.J. Kim, R.J. Birgeneau, M.A. Kastner, Y.S. Lee, Y. Endoh, G. Shirane, and K. Yamada, Phys. Rev. B **60**, 3294 (1999).
[91] T. Sato, T. Yokoya, Y. Naitoh, T. Takahashi, K. Yamada, and Y. Endoh, Phys. Rev. Lett. **83**, 2254 (1999).
[92] X.J. Zhou, P. Bogdanov, S.A. Kellar, T. Noda, H. Eisaki, S. Uchida, Z. Hussain, and Z.-X. Shen, Science **286**, 268 (1999).

[93] D.L. Feng, W.J. Zheng, K.M. Shen, D.H. Lu, F. Ronning, J.-I. Shimoyama, K. Kishio, G. Gu, D. Van der Marel, and Z.-X. Shen, cond-mat/9908056 (unpublished).
[94] H.M. Fretwell, A. Kaminski, J. Mesot, J.C. Campuzano, M.R. Norman, M. Randeria, T. Sato, R. Gatt, T. Takahashi, and K. Kadowaki, Phys. Rev. Lett. **84**, 4449 (2000); J. Mesot, A. Kaminski, H.M. Fretwell, M. Randeria, J.C. Campuzano, H. Ding, M.R. Norman, T. Takeuchi, T. Sato, T. Yokoya, T. Takahashi, I. Chong, T. Terashima, M. Takano, T. Mochiku, and K. Kadowaki, cond-mat/9910430 (unpublished).
[95] C. Kusko and R.S. Markiewicz, Phys. Rev. Lett. **84**, 963 (2000).
[96] G. Aeppli, T.E. Mason, S.M. Hayden, H.A. Mook, and J. Culda, Science **278**, 1432 (1997).
[97] G.S. Boebinger, Y. Ando, A. Passner, T. Kimura, M. Okuya, J. Shimoyama, K. Kishio, K. Tamasaku, N. Ichikawa, and S. Uchida, Phys. Rev. Lett. **77**, 5417 (1996).
[98] D.S. Marshall, D.S. Dessau, A.G. Loeser, C.-H. Park, A.Y. Matsuura, J.N. Eckstein, I. Bozovic, P. Fournier, A. Kapitulnik, W.E. Spicer, and Z.-X. Shen, Phys. Rev. Lett. **76**, 4841 (1996).
[99] G.B. Teitel'baum, B. Büchner, and H. de Gronckel, cond-mat/0005090 [Proceedings of the 6th International Conference on Materials and Mechanisms of Superconductivity, Houston, TX, February, 2000, Physica C (to be published)].
[100] J. Orenstein and A.J. Millis, Science **288**, 468 (2000).
[101] P.A. Lee and X.G. Wen, Phys. Rev. Lett. **78**, 4111 (1997).
[102] R.S. Markiewicz, Bull. Am. Phys. Soc. **43**, 320 (1998); R.S. Markiewicz, C. Kusko, and M.T. Vaughn, *ibid.* **44**(1), 460 (1999).